

FEATURES

- Wide gain bandwidth product: 18 MHz typical**
- High slew rate: 48 V/μs typical**
- Low voltage noise density: 3.3 nV/√Hz typical at 1 kHz**
- Low peak-to-peak noise: 0.15 μV p-p, 0.1 Hz to 10 Hz**
- Low input bias current: ±15 pA typical at T_A = 25°C**
- Low offset voltage: ±80 μV maximum at T_A = 25°C**
- Offset voltage drift: ±1.2 μV/°C maximum at T_A = -40°C to 85°C**
- Fast settling: 0.01% in 700 ns typical**
- Wide range of operating voltages**
 - Dual-supply operation: ±2.5 V to ±18 V**
 - Single-supply operation: 5 V to 36 V**
- Input voltage range includes V-**
- Rail-to-rail output**
- High capacitive load drive capability**
- Output short-circuit current: ±46 mA**
- No phase reversal**
- Unity-gain stable**

APPLICATIONS

- PLL filter amplifiers**
- Transimpedance amplifiers**
- Photodiode sensor interfaces**
- Low noise charge amplifiers**

GENERAL DESCRIPTION

The ADA4625-1/ADA4625-2 build on Analog Devices, Inc., high voltage, single-supply, rail-to-rail output (RRO), precision junction field effect transistor (JFET) input op amps, taking that product type to a level of speed and low noise that has not been made available to the market previously.

The ADA4625-1/ADA4625-2 provide optimal performance in high voltage, high gain, and low noise applications. The input common-mode voltage range includes the negative supply, and the output swings rail to rail. This enables the user to maximize dynamic input range in low voltage, single supply applications without the need for a separate negative voltage power supply for ground sense.

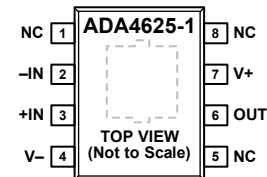
The combination of wide bandwidth, low noise, and low input bias current makes the ADA4625-1/ADA4625-2 especially suitable for phase-locked loop (PLL), active filter amplifiers and for high tuning voltage (V_{TUNE}), voltage controlled oscillators (VCOs) and preamplifiers where low level signals require an amplifier that provides both high amplification and wide bandwidth.

Rev. A

[Document Feedback](#)

Information furnished by Analog Devices is believed to be accurate and reliable. However, no responsibility is assumed by Analog Devices for its use, nor for any infringements of patents or other rights of third parties that may result from its use. Specifications subject to change without notice. No license is granted by implication or otherwise under any patent or patent rights of Analog Devices. Trademarks and registered trademarks are the property of their respective owners.

PIN CONFIGURATION



NOTES

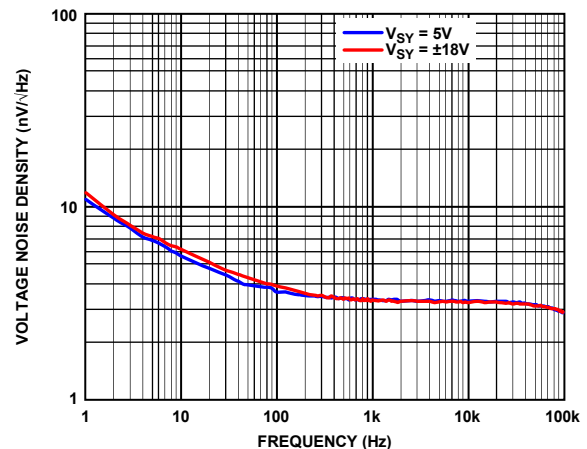
1. NC = NO CONNECTION. DO NOT CONNECT TO THIS PIN.
2. EXPOSED PAD. CONNECT THE EXPOSED PAD TO GND, V+ OR V- PLANE, OR LEAVE IT FLOATING.

15893-001

Figure 1.

The ADA4625-1/ADA4625-2 are unity-gain stable, and there is no phase reversal when input range exceeds either supply rail by 200 mV. The output is capable of driving loads up to 1000 pF and/or 600 Ω loads.

The ADA4625-1/ADA4625-2 are specified for operation over the extended industrial temperature range of -40°C to +125°C and operates from +5 V to +36 V (±2.5 V to ±18 V) with specifications at +5 V and ±18 V. The devices are available in an 8-lead SOIC package with an exposed pad (EPAD).



15893-157

Figure 2. Voltage Noise Density vs. Frequency

Table 1. Related Precision JFET Operational Amplifiers

Single	Dual	Quad
Not applicable	AD823A	Not applicable
AD8510	AD8512	AD8513
AD8610	AD8620	Not applicable
ADA4610-1	ADA4610-2	ADA4610-4
ADA4622-1	ADA4622-2	ADA4622-4
ADA4627-1/ADA4637-1	Not applicable	Not applicable

TABLE OF CONTENTS

Features	1
Applications	1
General Description	1
Pin Configuration	1
Revision History	2
Specifications	3
Electrical Characteristics— ± 18 V Operation	3
Electrical Characteristics—5 V Operation	5
Absolute Maximum Ratings	7
Thermal Resistance	7
ESD Caution	7
Pin Configurations and Function Descriptions	8
Typical Performance Characteristics	9
Theory of Operation	23
Input and Gain Stages	23

REVISION HISTORY

6/2019—Rev. 0 to Rev. A

Added ADA4625-2	Throughout
Changes to Table 2	3
Changes to Table 3	5
Added Figure 4 and Table 7; Renumbered Sequentially	8
Changes to Table 6	8
Added Figure 16	10
Added Figure 25 and Figure 28	12
Added Figure 17, Figure 38, and Figure 40	14
Added Figure 61 and Figure 64	18
Added Figure 65 to Figure 70	19
Added Figure 73 and Figure 76	20

Output Stage	23
No Phase Inversion	24
Supply Current	24
Applications Information	25
Active Loop Filter for Phase-Locked Loops (PLLs)	25
ADA4625-1 Advantages and Design Example	26
Transimpedance Amplifier	27
DAC Output Driver	31
Recommended Power Solution	32
Input Overvoltage Protection	32
Driving Capacitive Loads	32
Thermal Management	32
Typical Applications	33
Outline Dimensions	35
Ordering Guide	35

Added Figure 77 and Figure 80	21
Added Figure 84	22
Added DAC Output Driver Section, Figure 105, Figure 106, and Figure 107	31
Added Typical Applications Section, Figure 109, and Figure 110	33
Added Figure 111 and Figure 112	34
Updated Outline Dimensions	35
Changes to Ordering Guide	35

10/2017—Revision 0: Initial Version

SPECIFICATIONS

ELECTRICAL CHARACTERISTICS—±18 V OPERATION

Supply voltage (V_{SY}) = ±18 V, common-mode voltage (V_{CM}) = output voltage (V_{OUT}) = 0 V, T_A = 25°C, unless otherwise noted.

Table 2.

Parameter	Symbol	Test Conditions/Comments	Min	Typ	Max	Unit
INPUT CHARACTERISTICS						
Offset Voltage	V_{OS}	ADA4625-1		±15	±80	μV
		ADA4625-2			±100	μV
Offset Voltage Drift	TCV_{OS}	−40°C < T_A < +125°C			±250	μV
		−40°C < T_A < +85°C		±0.2	±1.2	μV/°C
Input Bias Current	I_B	−40°C < T_A < +125°C		±0.5	±2.1	μV/°C
		−40°C < T_A < +125°C		±15	±75	pA
Input Offset Current	I_{OS}	ADA4625-1, −40°C < T_A < +125°C			±5.5	nA
		ADA4625-2, −40°C < T_A < +125°C			±7	nA
Input Voltage Range	IVR	ADA4625-1, −40°C < T_A < +125°C			±0.4	nA
		ADA4625-2, −40°C < T_A < +125°C			±0.7	nA
Common-Mode Rejection Ratio	CMRR	V_{CM} = −18.2 V to +14.5 V	−18.2		+14.5	V
		−40°C < T_A < +125°C	97	115		dB
		V_{CM} = −18.2 V to +12 V	94			dB
		−40°C < T_A < +125°C	115	130		dB
		−40°C < T_A < +125°C	110			dB
Large Signal Voltage Gain	A_{VO}	Load resistance (R_L) = 2 kΩ, V_{OUT} = −17.5 V to +17.5 V	140	150		dB
		−40°C < T_A < +125°C	135			dB
		R_L = 600 Ω, V_{OUT} = −15 V to +15 V	130	135		dB
		ADA4625-1, −40°C < T_A < +125°C	115			dB
		ADA4625-2, −40°C < T_A < +125°C	100			dB
Input Capacitance	C_{DM}	ADA4625-1		8.6		pF
		ADA4625-2		13.8		pF
Common Mode	C_{CM}	ADA4625-1		11.3		pF
		ADA4625-2		13.3		pF
Input Resistance	R_{DM}	Differential mode		10^{12}		Ω
	R_{CM}	Common mode, V_{CM} from −18 V to +12 V		10^{12}		Ω
OUTPUT CHARACTERISTICS						
Output Voltage High	V_{OH}	R_L = 2 kΩ	17.65	17.72		V
		−40°C < T_A < +125°C	17.5			V
		R_L = 600 Ω	17.0	17.28		V
		−40°C < T_A < +125°C	16.75			V
Output Voltage Low	V_{OL}	R_L = 2 kΩ		−17.74	−17.70	V
		−40°C < T_A < +125°C			−17.5	V
		R_L = 600 Ω		−17.4	−17.0	V
		−40°C < T_A < +125°C			−16.85	V
Output Current	I_{OUT}	Dropout voltage ($V_{DROPOUT}$) < 1 V		±33		mA
Short-Circuit Current	I_{SC}			±46		mA
Closed-Loop Output Impedance	Z_{OUT}	f = 1 MHz, closed-loop gain (A_V) = +1		2		Ω
		A_V = +10		18		Ω
		A_V = +100		29		Ω
POWER SUPPLY						
Power Supply Rejection Ratio	PSRR	V_{SY} = ±5 V to ±18 V	105	120		dB
		−40°C < T_A < +125°C	102			dB
Supply Current per Amplifier	I_{SY}	V_{OUT} = 0 V		4.0	4.5	mA
		−40°C < T_A < +125°C			5	mA

Parameter	Symbol	Test Conditions/Comments	Min	Typ	Max	Unit
DYNAMIC PERFORMANCE						
Slew Rate	SR	$V_{OUT} = \pm 10\text{ V}$, $R_L = 2\text{ k}\Omega$, $A_V = -1$ $V_{OUT} = \pm 10\text{ V}$, $R_L = 2\text{ k}\Omega$, $A_V = -5$		48 44		V/ μ s V/ μ s
Gain Bandwidth Product	GBP	$A_V = 100$		18		MHz
Unity-Gain Crossover	UGC	$A_V = 1$		12.4		MHz
-3 dB Bandwidth	-3 dB	$A_V = 1$		16		MHz
Phase Margin	Φ_M	ADA4625-1		88		Degrees
		ADA4625-2		75		Degrees
Channel Separation	CS	$V_{IN} = 15\text{ V p-p}$, $f = 1\text{ kHz}$, $R_L = 2\text{ k}\Omega$, $A_V = 100$ $V_{IN} = 15\text{ V p-p}$, $f = 10\text{ kHz}$, $R_L = 2\text{ k}\Omega$, $A_V = 100$		108 88		dB dB
Settling Time	t_s	To 0.1%, input voltage (V_{IN}) = 10 V step, $R_L = 2\text{ k}\Omega$, load capacitance (C_L) = 15 pF, $A_V = -1$ To 0.01%, $V_{IN} = 10\text{ V}$ step, $R_L = 2\text{ k}\Omega$, $C_L = 15\text{ pF}$, $A_V = -1$		500 700		ns ns
ADA4625-1		To 0.1%, $V_{IN} = 10\text{ V}$ step, $R_L = 2\text{ k}\Omega$, $C_L = 15\text{ pF}$, $A_V = -1$ To 0.01%, $V_{IN} = 10\text{ V}$ step, $R_L = 2\text{ k}\Omega$, $C_L = 15\text{ pF}$, $A_V = -1$		700 1200		ns ns
ADA4625-2		To 0.1%, $V_{IN} = 10\text{ V}$ step, $R_L = 2\text{ k}\Omega$, $C_L = 15\text{ pF}$, $A_V = -1$ To 0.01%, $V_{IN} = 10\text{ V}$ step, $R_L = 2\text{ k}\Omega$, $C_L = 15\text{ pF}$, $A_V = -1$		1200		ns
ELECTROMAGNETIC INTERFERENCE (EMI) REJECTION RATIO						
f = 1000 MHz	EMIRR	ADA4625-1/ADA4625-2		56		dB
f = 2400 MHz		ADA4625-1		93		dB
		ADA4625-2		73		dB
NOISE PERFORMANCE						
Peak-to-Peak Noise	e_N p-p	0.1 Hz to 10 Hz		0.15		μ V p-p
Voltage Noise Density	e_N	f = 10 Hz f = 100 Hz f = 1 kHz		5.5 3.6 3.3		nV/ $\sqrt{\text{Hz}}$ nV/ $\sqrt{\text{Hz}}$ nV/ $\sqrt{\text{Hz}}$
Current Noise Density	i_N	f = 1 kHz		4.5		fA/ $\sqrt{\text{Hz}}$
Total Harmonic Distortion + Noise	THD + N	$A_V = 1$, f = 10 Hz to 20 kHz, $R_L = 2\text{ k}\Omega$, $V_{IN} = 6\text{ V}_{RMS}$ at 1 kHz				
Bandwidth = 80 kHz				0.0003		%
				-109		dB
Bandwidth = 500 kHz				0.0007		%
				-103		dB

ELECTRICAL CHARACTERISTICS—5 V OPERATION

$V_{SY} = 5\text{ V}$, $V_{CM} = 1.5\text{ V}$, $V_{OUT} = V_{SY}/2$, $T_A = 25^\circ\text{C}$, unless otherwise noted.

Table 3.

Parameter	Symbol	Test Conditions/Comments	Min	Typ	Max	Unit
INPUT CHARACTERISTICS						
Offset Voltage	V_{OS}	$-40^\circ\text{C} < T_A < +125^\circ\text{C}$		± 0.1	± 0.6	mV
Offset Voltage Drift	TCV_{OS}	ADA4625-1, $-40^\circ\text{C} < T_A < +85^\circ\text{C}$		± 0.4	± 1.0	mV
		ADA4625-2, $-40^\circ\text{C} < T_A < +85^\circ\text{C}$			± 2.6	$\mu\text{V}/^\circ\text{C}$
Input Bias Current	I_B	ADA4625-1, $-40^\circ\text{C} < T_A < +125^\circ\text{C}$		± 0.7	± 3.6	$\mu\text{V}/^\circ\text{C}$
		ADA4625-2, $-40^\circ\text{C} < T_A < +125^\circ\text{C}$			± 4.5	$\mu\text{V}/^\circ\text{C}$
Input Offset Current	I_{OS}	ADA4625-1, $-40^\circ\text{C} < T_A < +125^\circ\text{C}$		± 15	± 50	pA
		ADA4625-2, $-40^\circ\text{C} < T_A < +125^\circ\text{C}$			± 3.5	nA
Input Voltage Range	IVR	$-40^\circ\text{C} < T_A < +125^\circ\text{C}$		± 2	± 50	pA
					± 150	pA
Common-Mode Rejection Ratio	CMRR	$V_{CM} = 0\text{ V to } 1.5\text{ V}$ $-40^\circ\text{C} < T_A < +125^\circ\text{C}$	74	90		dB
Large Signal Voltage Gain	A_{VO}	$R_L = 2\text{ k}\Omega$ to V_- , $V_{OUT} = 0.35\text{ V to } 4.65\text{ V}$ $-40^\circ\text{C} < T_A < +125^\circ\text{C}$	70			dB
		$R_L = 600\ \Omega$ to V_- , $V_{OUT} = 0.5\text{ V to } 4.5\text{ V}$ $-40^\circ\text{C} < T_A < +125^\circ\text{C}$	130	145		dB
		$R_L = 600\ \Omega$ to V_- , $V_{OUT} = 0.5\text{ V to } 4.5\text{ V}$ $-40^\circ\text{C} < T_A < +125^\circ\text{C}$	120			dB
		$R_L = 600\ \Omega$ to V_- , $V_{OUT} = 0.5\text{ V to } 4.5\text{ V}$ $-40^\circ\text{C} < T_A < +125^\circ\text{C}$	120	130		dB
Input Capacitance Differential Mode	C_{DM}	ADA4625-1		12.1		pF
		ADA4625-2		12.7		pF
Common Mode	C_{CM}	ADA4625-1		16.3		pF
		ADA4625-2		18.4		pF
Input Resistance	R_{DM} R_{CM}	Differential mode		10^{12}		Ω
		Common mode, V_{CM} from 0 V to 1.5 V		10^{12}		Ω
OUTPUT CHARACTERISTICS						
Output Voltage High	V_{OH}	$R_L = 2\text{ k}\Omega$ to V_- $-40^\circ\text{C} < T_A < +125^\circ\text{C}$	4.75	4.82		V
		$R_L = 600\ \Omega$ to V_- $-40^\circ\text{C} < T_A < +125^\circ\text{C}$	4.7			V
		$R_L = 600\ \Omega$ to V_- $-40^\circ\text{C} < T_A < +125^\circ\text{C}$	4.65	4.74		V
		$R_L = 600\ \Omega$ to V_- $-40^\circ\text{C} < T_A < +125^\circ\text{C}$	4.55			V
Output Voltage Low	V_{OL}	$R_L = 2\text{ k}\Omega$ to V_+ $-40^\circ\text{C} < T_A < +125^\circ\text{C}$		0.17	0.22	V
		$R_L = 600\ \Omega$ to V_+ $-40^\circ\text{C} < T_A < +125^\circ\text{C}$			0.3	V
		$R_L = 600\ \Omega$ to V_+ $-40^\circ\text{C} < T_A < +125^\circ\text{C}$		0.25	0.3	V
		$R_L = 600\ \Omega$ to V_+ $-40^\circ\text{C} < T_A < +125^\circ\text{C}$			0.45	V
Output Current	I_{OUT}	$V_{DROPOUT} < 1\text{ V}$		± 33		mA
Short-Circuit Current	I_{SC}			± 46		mA
Closed-Loop Output Impedance	Z_{OUT}	$f = 1\text{ MHz}$, $A_V = +1$		2		Ω
		$A_V = +10$		18		Ω
		$A_V = +100$		29		Ω
POWER SUPPLY						
Power Supply Rejection Ratio	PSRR	$V_{SY} = 4.5\text{ V to } 10\text{ V}$ $-40^\circ\text{C} < T_A < +125^\circ\text{C}$	80	97		dB
Supply Current per Amplifier	I_{SY}	$V_{OUT} = 0\text{ V}$				dB
		$-40^\circ\text{C} < T_A < +125^\circ\text{C}$		3.9	4.3	mA
					4.8	mA

Parameter	Symbol	Test Conditions/Comments	Min	Typ	Max	Unit	
DYNAMIC PERFORMANCE							
Slew Rate	SR	$V_{OUT} = 0.5\text{ V to }4.5\text{ V}, R_L = 2\text{ k}\Omega, A_V = -1$		32		V/ μ s	
		$V_{OUT} = 0.5\text{ V to }4.5\text{ V}, R_L = 2\text{ k}\Omega, A_V = -5$		27		V/ μ s	
Gain Bandwidth Product	GBP	$A_V = 100$		16		MHz	
Unity-Gain Crossover	UGC	$A_V = 1$		11.2		MHz	
-3 dB Bandwidth	-3 dB	$A_V = 1$		16		MHz	
Phase Margin	Φ_M	ADA4625-1		86		Degrees	
		ADA4625-2		71		Degrees	
Channel Separation	CS	$V_{IN} = 15\text{ V p-p}, f = 1\text{ kHz}, R_L = 2\text{ k}\Omega, A_V = 100$		108		dB	
		$V_{IN} = 15\text{ V p-p}, f = 100\text{ kHz}, R_L = 2\text{ k}\Omega, A_V = 100$		88		dB	
Settling Time	t_s	To 0.1%, $V_{IN} = 4\text{ V step}, R_L = 2\text{ k}\Omega, C_L = 15\text{ pF}, A_V = -1$ To 0.01%, $V_{IN} = 4\text{ V step}, R_L = 2\text{ k}\Omega, C_L = 15\text{ pF}, A_V = -1$		600		ns	
					950		ns
					1250		ns
					1350		ns
EMI REJECTION RATIO	EMIRR	ADA4625-1/ADA4625-2		56		dB	
			f = 1000 MHz		87		dB
			f = 2400 MHz		79		dB
NOISE PERFORMANCE							
Peak-to-Peak Noise	$e_N\text{ p-p}$	0.1 Hz to 10 Hz		0.15		μ V p-p	
Voltage Noise Density	e_N	f = 10 Hz		5.5		nV/ $\sqrt{\text{Hz}}$	
		f = 100 Hz		3.6		nV/ $\sqrt{\text{Hz}}$	
		f = 1 kHz		3.3		nV/ $\sqrt{\text{Hz}}$	
		f = 1 kHz		4.5		fA/ $\sqrt{\text{Hz}}$	
Current Noise Density	i_N	f = 1 kHz		4.5		fA/ $\sqrt{\text{Hz}}$	
Total Harmonic Distortion + Noise	THD + N	$A_V = 1, f = 10\text{ Hz to }20\text{ kHz}, R_L = 2\text{ k}\Omega, V_{IN} = 0.6\text{ V}_{RMS}\text{ at }1\text{ kHz}$					
			ADA4625-1		0.0003		%
					-109		dB
			ADA4625-2		0.002		%
					-93		dB
			Bandwidth = 80 kHz				
Bandwidth = 500 kHz				0.0007		%	
					-103		dB
			ADA4625-1		0.0007		%
					-103		dB
				0.004		%	
				-89		dB	

ABSOLUTE MAXIMUM RATINGS

Table 4.

Parameter	Rating
Supply Voltage	40 V
Input Voltage	(V ₋) - 0.2 V to (V ₊) + 0.2 V
Differential Input Voltage	(V ₋) - 0.2 V to (V ₊) + 0.2 V
Input Current ¹	±20 mA
Storage Temperature Range	-65°C to +150°C
Operating Temperature Range	-40°C to +125°C
Junction Temperature Range	-65°C to +150°C
Lead Temperature, Soldering (10 sec)	300°C
Electrostatic Discharge (ESD)	
Human Body Model (HBM) ²	
ADA4625-1	1.25 kV
ADA4625-2	1.5 kV
Field Induced Charge Device Model (FICDM) ³	
ADA4625-1	1.25 kV
ADA4625-2	1.25 kV

¹ The input pins have clamp diodes connected to the power supply pins. Limit the input current to 20 mA or less whenever input signals exceed the power supply rail by 0.3 V.

² ESDA/JEDEC JS-001-2011 applicable standard.

³ JESD22-C101 (ESD FICDM standard of JEDEC) applicable standard.

Stresses at or above those listed under Absolute Maximum Ratings may cause permanent damage to the product. This is a stress rating only; functional operation of the product at these or any other conditions above those indicated in the operational section of this specification is not implied. Operation beyond the maximum operating conditions for extended periods may affect product reliability.

THERMAL RESISTANCE

Thermal performance is directly linked to printed circuit board (PCB) design and operating environment. Close attention to PCB thermal design is required.

Table 5. Thermal Resistance

Package Type ^{1, 2}	θ_{JA} ³	θ_{JC}	Unit
RD-8-1	52.8	5.7	°C/W

¹ Values were obtained per JEDEC standard JESD-51.

² Although the exposed pad can be left floating, it must be connected to the GND, or the V₊ or V₋ plane for proper thermal management.

³ Board layout impacts thermal characteristics such as θ_{JA} . When proper thermal management techniques are used, a better θ_{JA} can be achieved. Refer to the Thermal Management section for additional information.

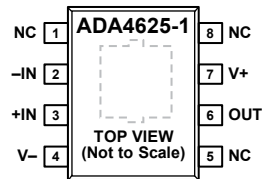
ESD CAUTION



ESD (electrostatic discharge) sensitive device.

Charged devices and circuit boards can discharge without detection. Although this product features patented or proprietary protection circuitry, damage may occur on devices subjected to high energy ESD. Therefore, proper ESD precautions should be taken to avoid performance degradation or loss of functionality.

PIN CONFIGURATIONS AND FUNCTION DESCRIPTIONS



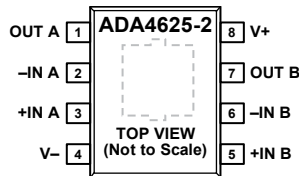
NOTES
 1. NC = NO CONNECTION. DO NOT CONNECT TO THIS PIN.
 2. EXPOSED PAD. CONNECT THE EXPOSED PAD TO GND, V+ OR V- PLANE, OR LEAVE IT FLOATING.

156893-002

Figure 3. ADA4625-1 Pin Configuration

Table 6. Pin Function Descriptions, ADA4625-1

Pin No.	Mnemonic	Description
1, 5, 8	NC	No Connection. Do not connect to these pins.
2	-IN	Inverting Input Pin.
3	+IN	Noninverting Input Pin.
4	V-	Negative Supply Voltage Pin.
6	OUT	Output Pin.
7	V+	Positive Supply Voltage Pin.
	EPAD	Exposed Pad. Connect the exposed pad to GND, V+ or V- plane, or leave it floating.



NOTES
 1. EXPOSED PAD. CONNECT THE EXPOSED PAD TO GND, V+ OR V- PLANE, OR LEAVE IT FLOATING.

156893-101

Figure 4. ADA4625-2 Pin Configuration

Table 7. Pin Function Descriptions, ADA4625-2

Pin No.	Mnemonic	Description
1	OUT A	Output Pin for Channel A.
2	-IN A	Inverting Input Pin for Channel A.
3	+IN A	Noninverting Input Pin for Channel A.
4	V-	Negative Supply Voltage Pin.
5	+IN B	Noninverting Input Pin for Channel B.
6	-IN B	Inverting Input Pin for Channel B.
7	OUT B	Output Pin for Channel B.
8	V+	Positive Supply Voltage Pin.
	EPAD	Exposed Pad. Connect the exposed pad to GND, V+ or V- plane, or leave it floating.

TYPICAL PERFORMANCE CHARACTERISTICS

$T_A = 25^\circ\text{C}$, $V_{CM} = 0\text{ V}$, unless otherwise noted.

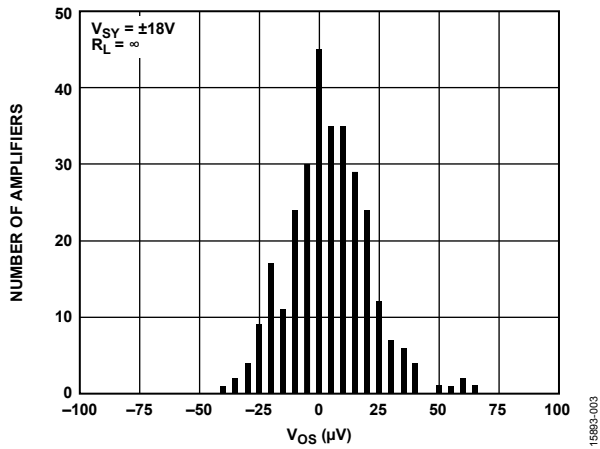


Figure 5. Input Offset Voltage (V_{OS}) Distribution, Supply Voltage (V_{SY}) = $\pm 18\text{ V}$

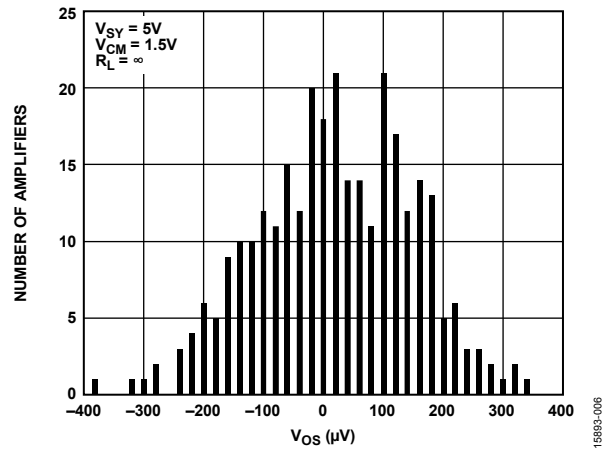


Figure 8. V_{OS} Distribution, $V_{SY} = 5\text{ V}$

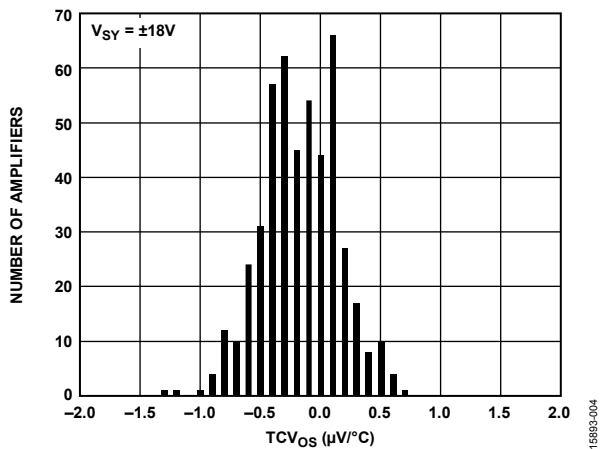


Figure 6. Input Offset Voltage Drift (TCV_{OS}) Distribution (-40°C to $+125^\circ\text{C}$), $V_{SY} = \pm 18\text{ V}$

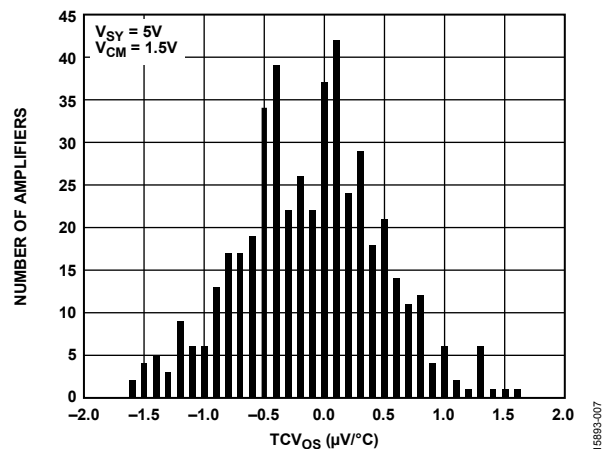


Figure 9. TCV_{OS} Distribution (-40°C to $+125^\circ\text{C}$), $V_{SY} = 5\text{ V}$

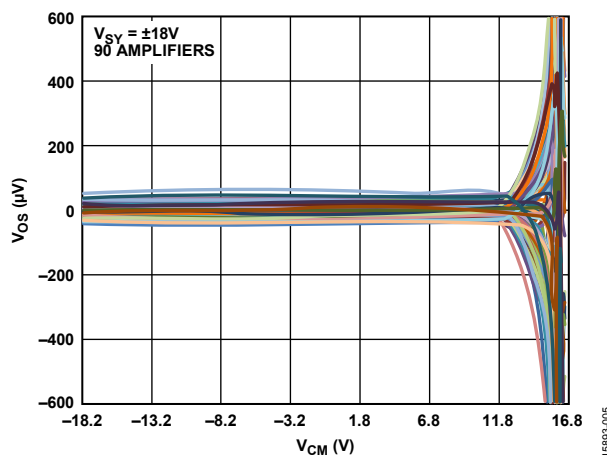


Figure 7. V_{OS} vs. Common-Mode Voltage (V_{CM}), $V_{SY} = \pm 18\text{ V}$

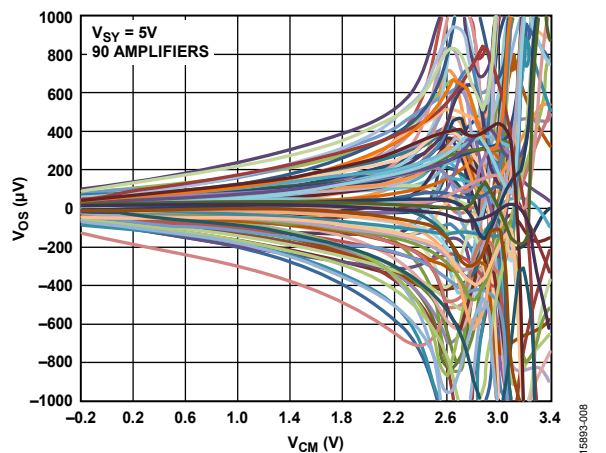


Figure 10. V_{OS} vs. V_{CM} , $V_{SY} = 5\text{ V}$

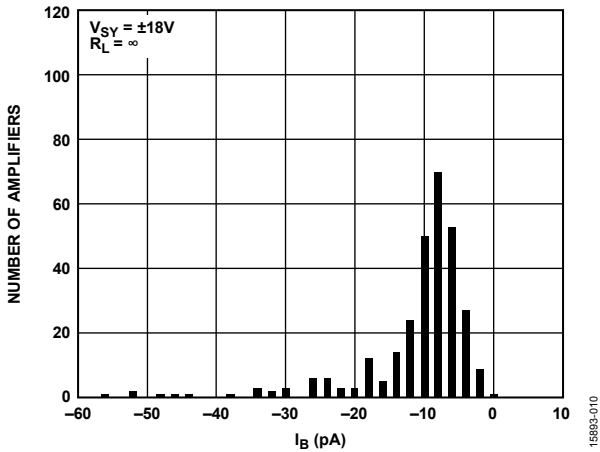


Figure 11. Input Bias Current (I_B) Distribution, $V_{SY} = \pm 18V$

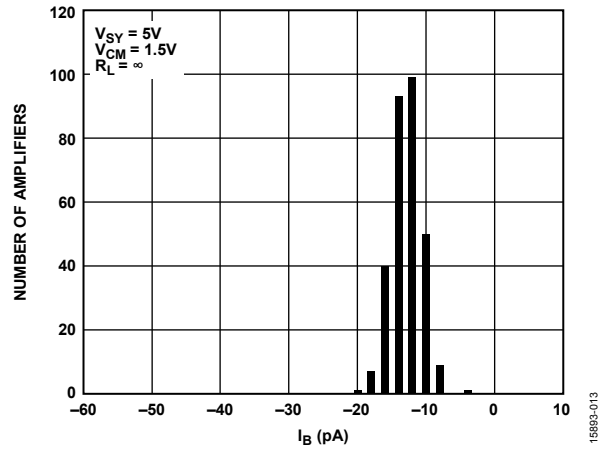


Figure 14. I_B Distribution, $V_{SY} = 5V$

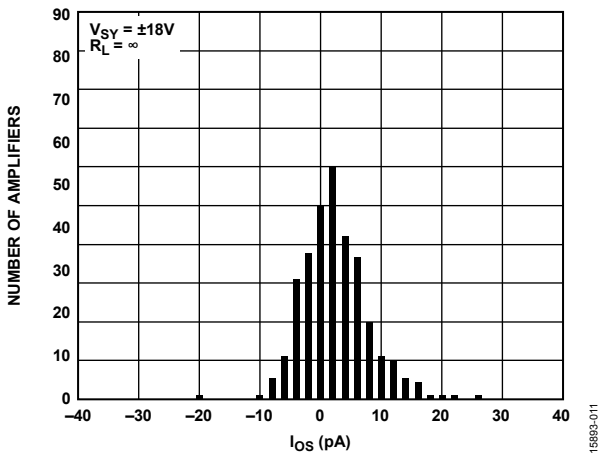


Figure 12. Input Offset Current (I_{OS}) Distribution, $V_{SY} = \pm 18V$

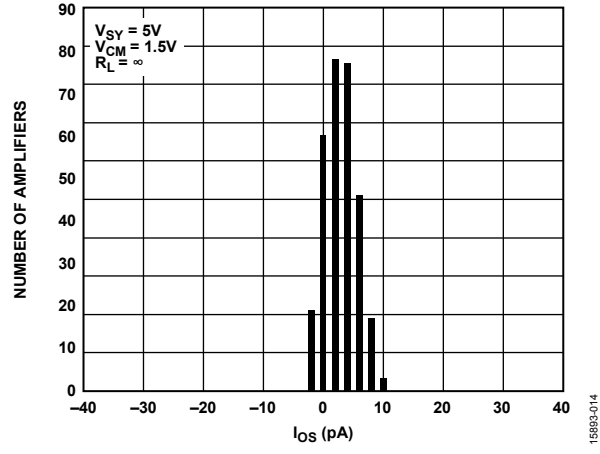


Figure 15. I_{OS} Distribution, $V_{SY} = 5V$

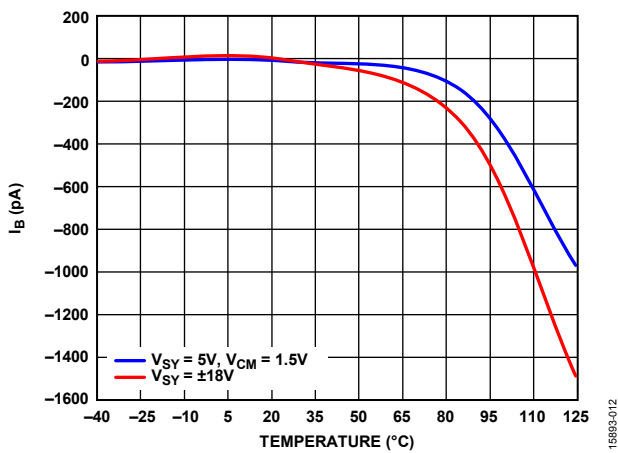


Figure 13. ADA4625-1 I_B vs. Temperature

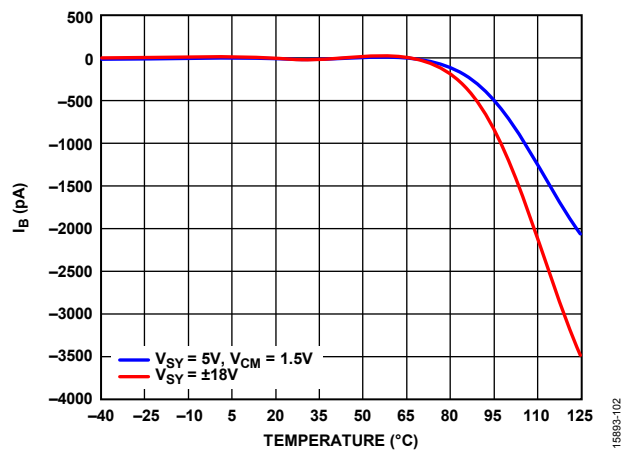


Figure 16. ADA4625-2 I_B vs. Temperature

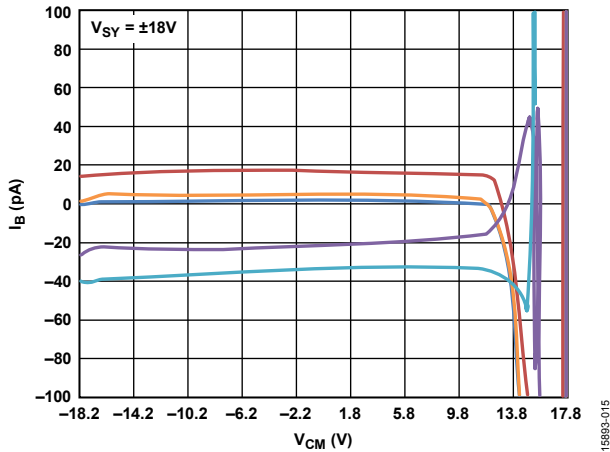


Figure 17. I_B vs. V_{CM} , $V_{SY} = \pm 18 V$

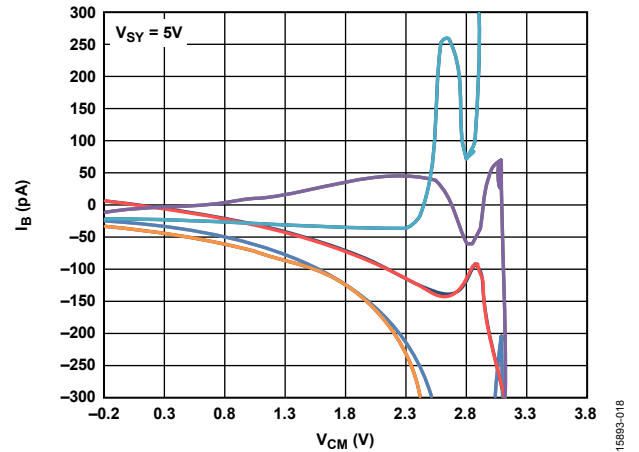


Figure 20. I_B vs. V_{CM} , $V_{SY} = 5 V$

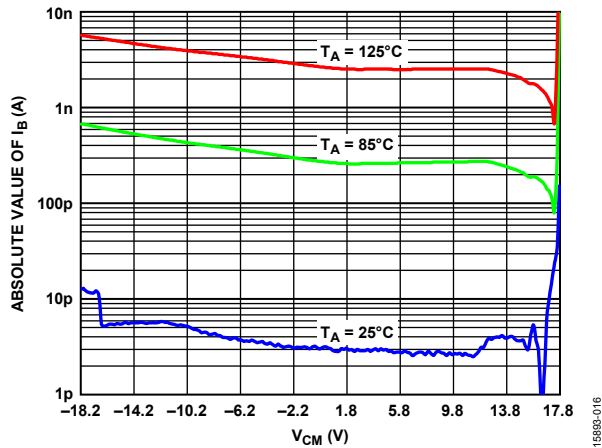


Figure 18. Absolute Value of I_B vs. V_{CM} for Various Temperatures, $V_{SY} = \pm 18 V$

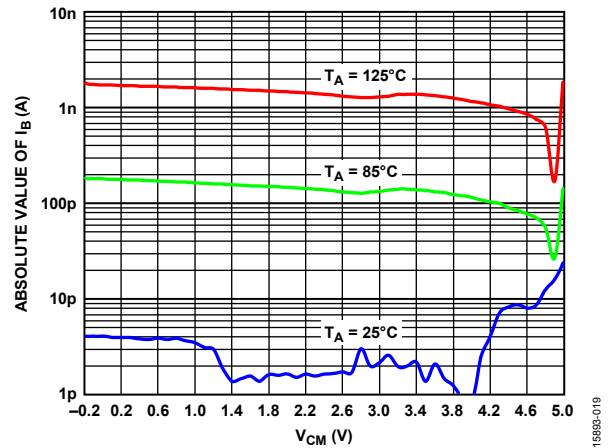


Figure 21. Absolute Value of I_B vs. V_{CM} for Various Temperature, $V_{SY} = 5 V$

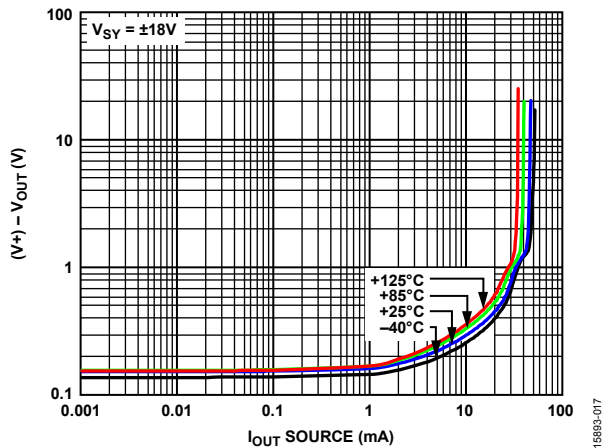


Figure 19. Dropout Voltage ($(V^+) - V_{OUT}$) vs. Output Current (I_{OUT}) Source for Various Temperatures, $V_{SY} = \pm 18 V$

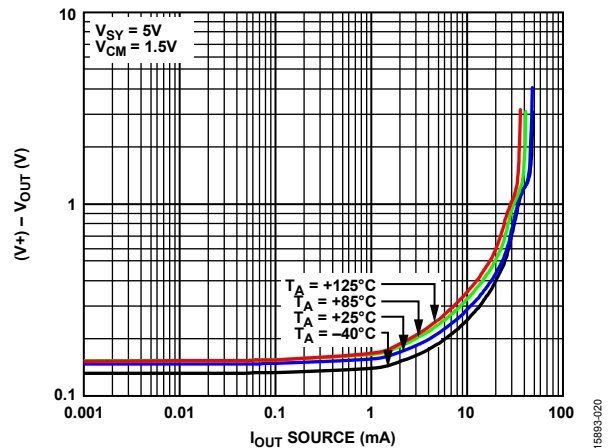


Figure 22. $(V^+) - V_{OUT}$ vs. I_{OUT} Source for Various Temperatures, $V_{SY} = 5 V$

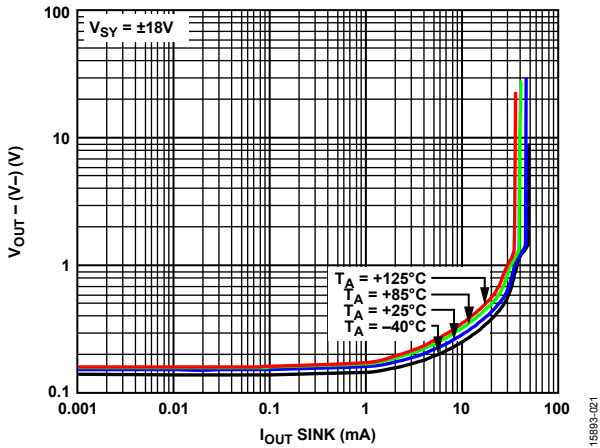


Figure 23. Dropout Voltage ($V_{OUT} - (V-)$) vs. I_{OUT} Sink for Various Temperatures, $V_{SY} = \pm 18 V$

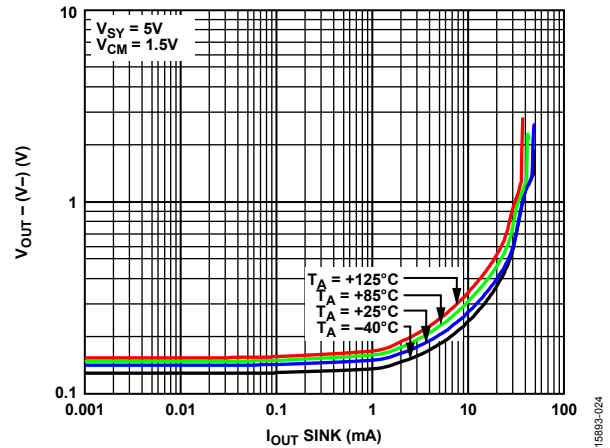


Figure 26. ($V_{OUT} - (V-)$) vs. I_{OUT} Sink for Various Temperatures, $V_{SY} = 5 V$

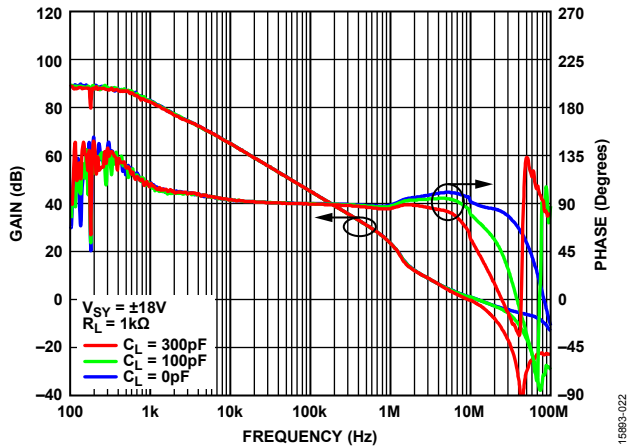


Figure 24. ADA4625-1 Open-Loop Gain and Phase vs. Frequency, $V_{SY} = \pm 18 V$

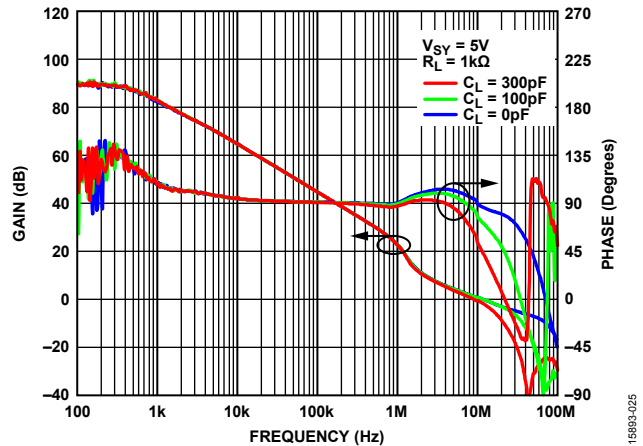


Figure 27. ADA4625-1 Open-Loop Gain and Phase vs. Frequency, $V_{SY} = 5 V$

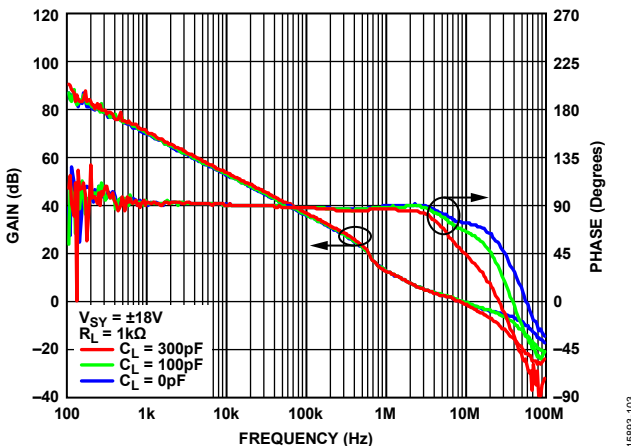


Figure 25. ADA4625-2 Open-Loop Gain and Phase vs. Frequency, $V_{SY} = \pm 18 V$

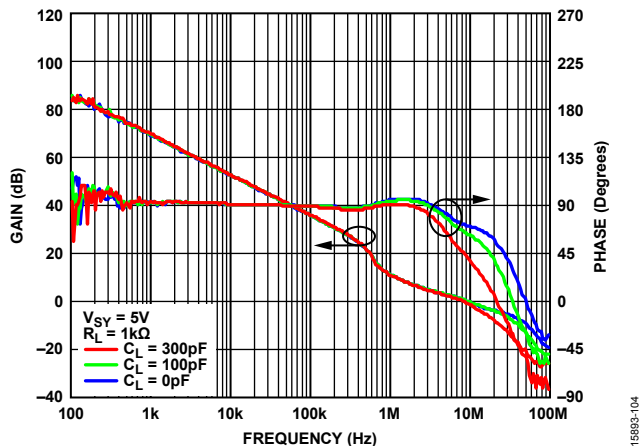


Figure 28. ADA4625-2 Open-Loop Gain and Phase vs. Frequency, $V_{SY} = 5 V$

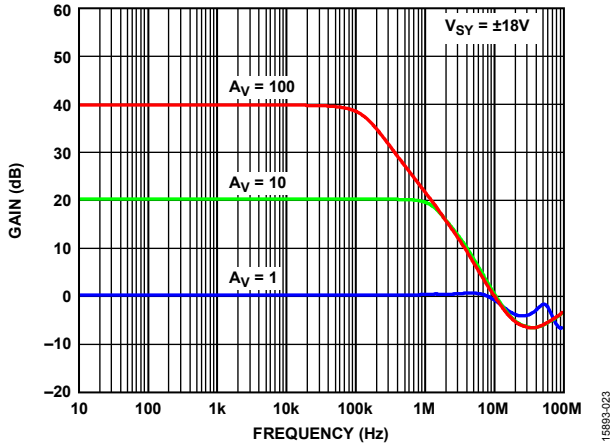


Figure 29. Gain vs. Frequency for Various Closed-Loop Gains, $V_{SY} = \pm 18V$

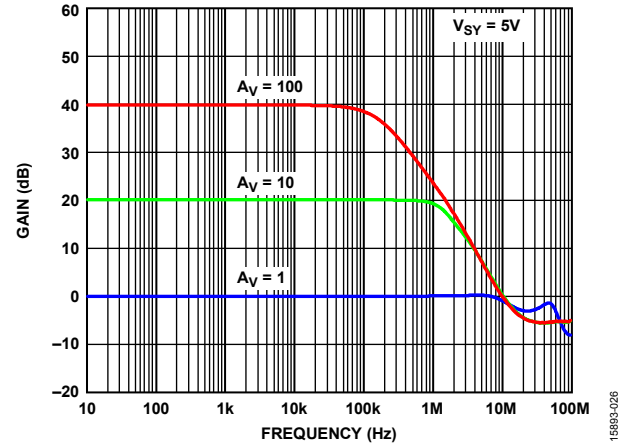


Figure 32. Gain vs. Frequency for Various Closed-Loop Gains, $V_{SY} = 5V$

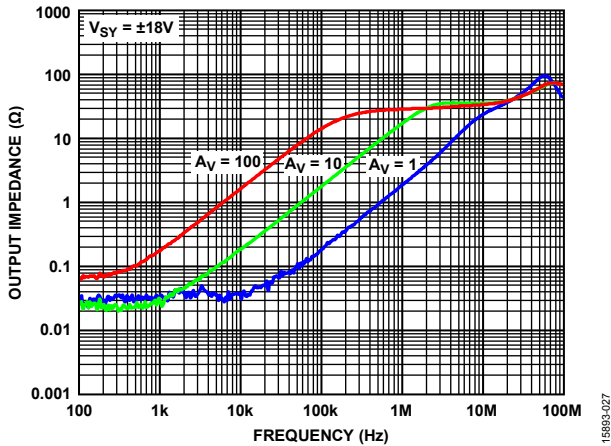


Figure 30. Output Impedance (Z_{OUT}) vs. Frequency, $V_{SY} = \pm 18V$

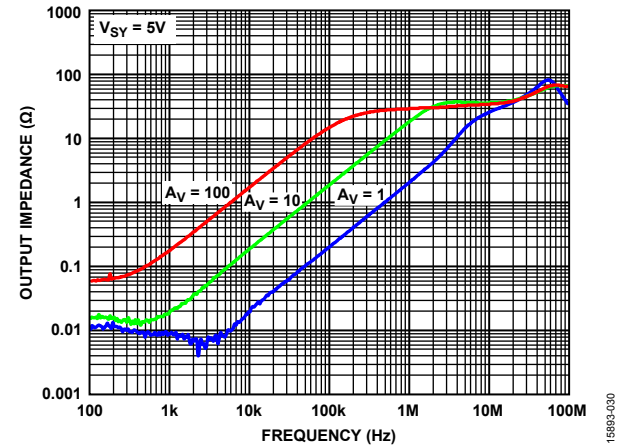


Figure 33. Z_{OUT} vs. Frequency, $V_{SY} = 5V$

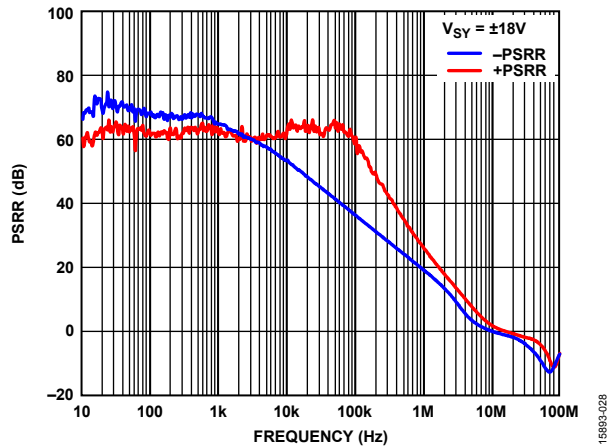


Figure 31. Power Supply Rejection Ratio (PSRR) vs. Frequency, $V_{SY} = \pm 18V$

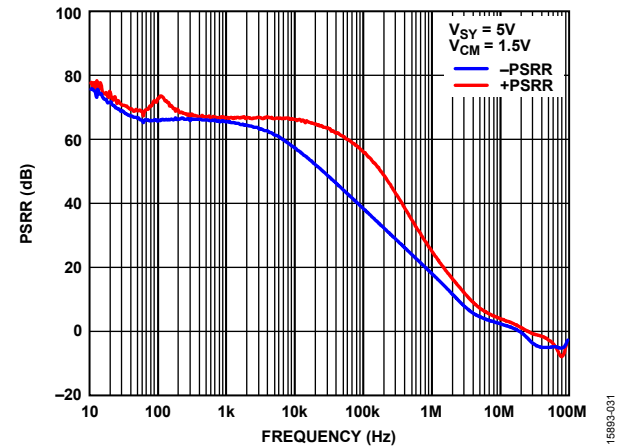


Figure 34. PSRR vs. Frequency, $V_{SY} = 5V$

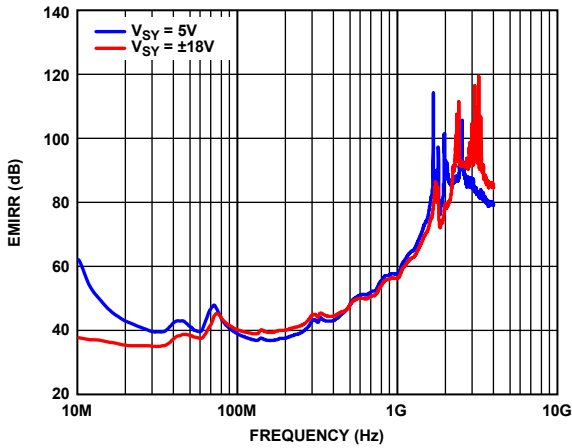


Figure 35. ADA4625-1 EMI Rejection Ratio (EMIRR) vs. Frequency

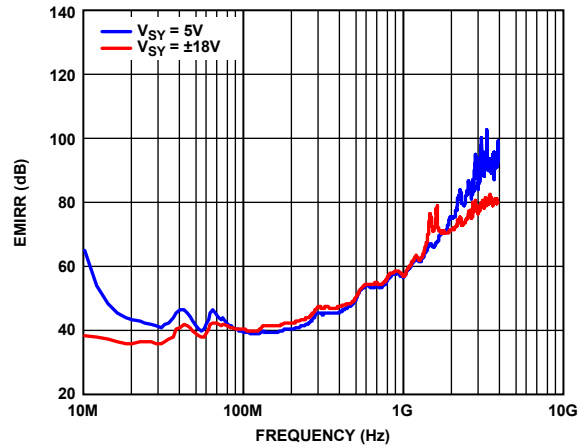


Figure 38. ADA4625-2 EMIRR vs. Frequency

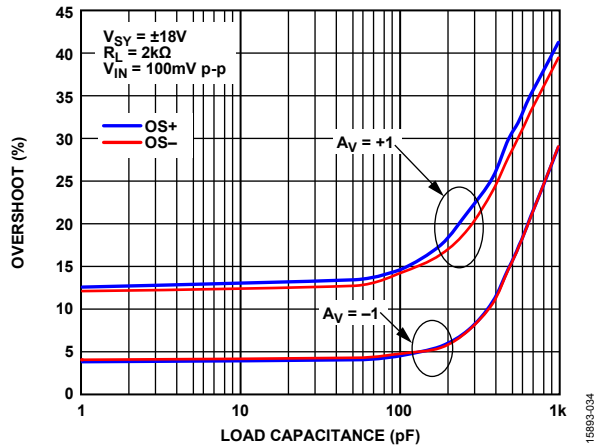


Figure 36. ADA4625-1 Small Signal Overshoot (OS±) vs. Load Capacitance, $V_{SY} = \pm 18 V$

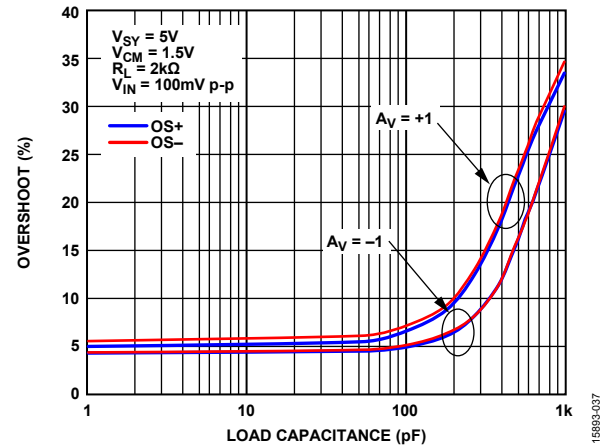


Figure 39. ADA4625-1 OS± vs. Load Capacitance, $V_{SY} = 5 V$

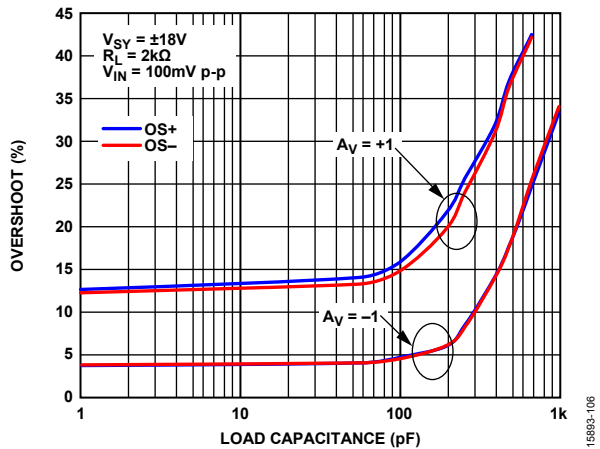


Figure 37. ADA4625-2 OS± vs. Load Capacitance, $V_{SY} = \pm 18 V$

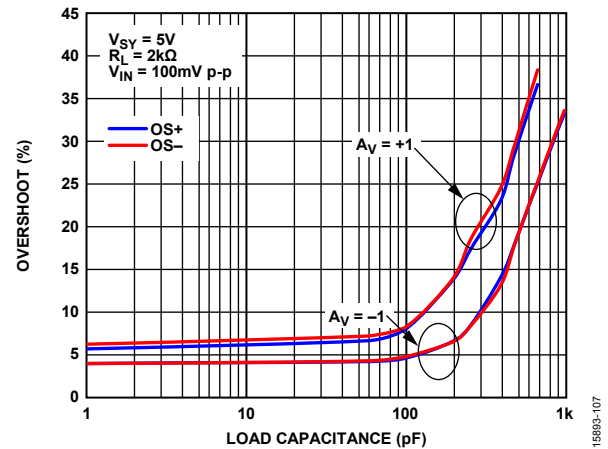


Figure 40. ADA4625-2 OS± vs. Load Capacitance, $V_{SY} = 5 V$

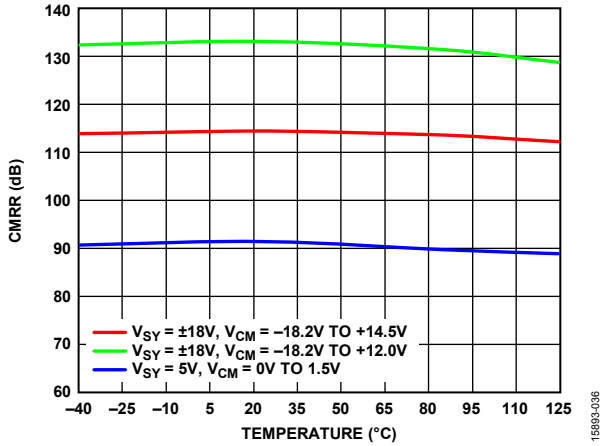


Figure 41. CMRR vs. Temperature

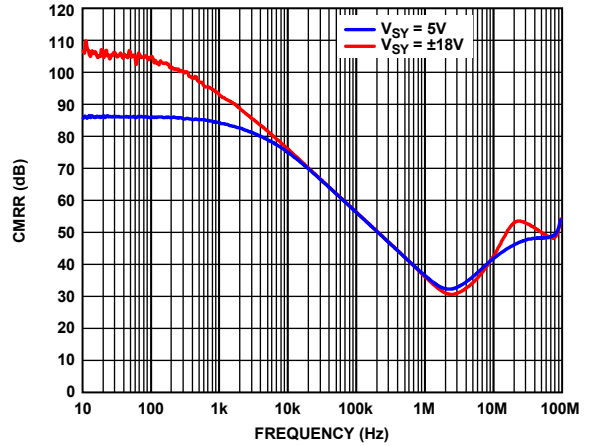


Figure 44. CMRR vs. Frequency

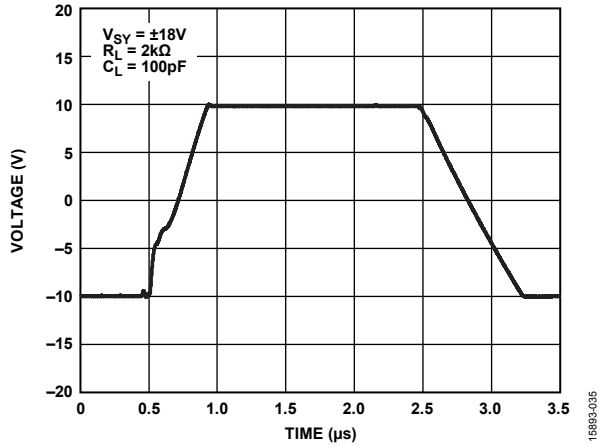


Figure 42. Large Signal Transient Response, $A_V = +1$, $V_{SY} = \pm 18 V$

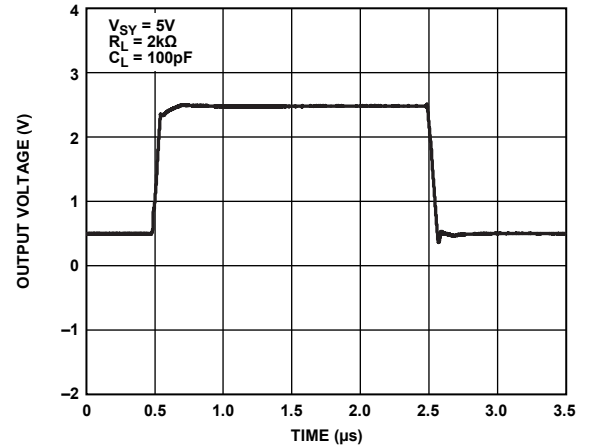


Figure 45. Large Signal Transient Response, $A_V = +1$, $V_{SY} = 5 V$

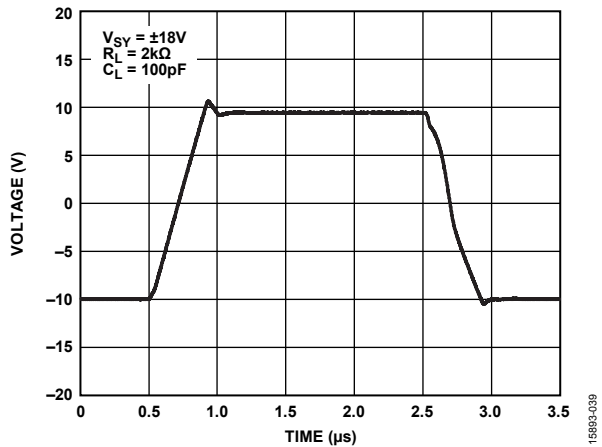


Figure 43. Large Signal Transient Response, $A_V = -1$, $V_{SY} = \pm 18 V$

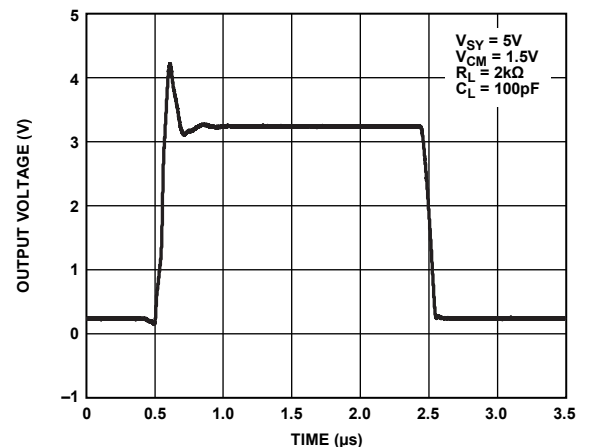


Figure 46. Large Signal Transient Response, $A_V = -1$, $V_{SY} = 5 V$

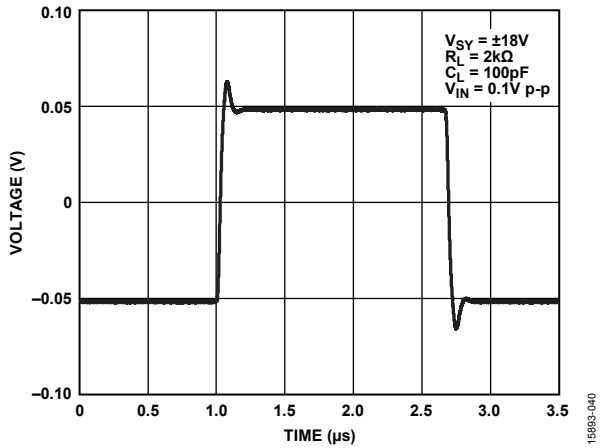


Figure 47. Small Signal Transient Response, $A_V = 1$, $V_{SY} = \pm 18\text{ V}$

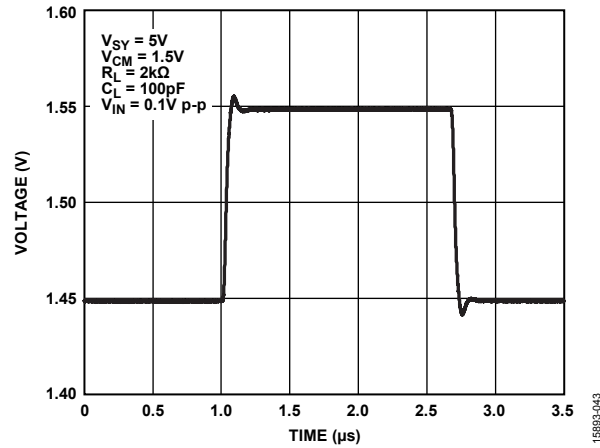


Figure 50. Small Signal Transient Response, $A_V = 1$, $V_{SY} = 5\text{ V}$

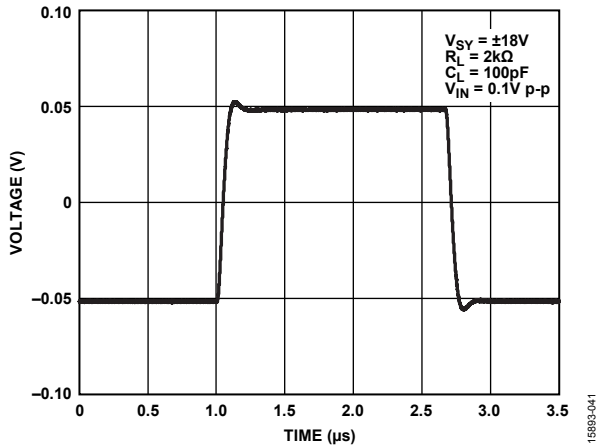


Figure 48. Small Signal Transient Response, $A_V = -1$, $V_{SY} = \pm 18\text{ V}$

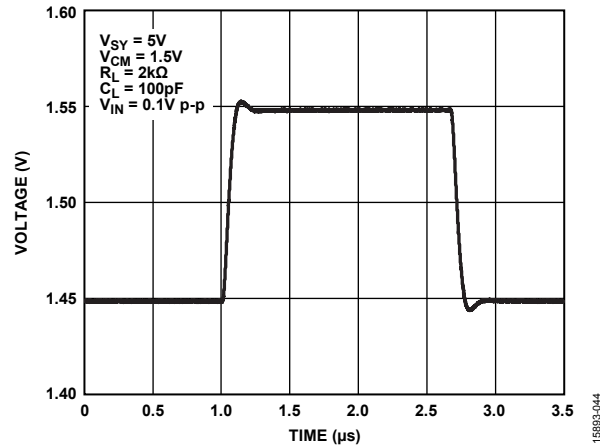


Figure 51. Small Signal Transient Response, $A_V = -1$, $V_{SY} = 5\text{ V}$

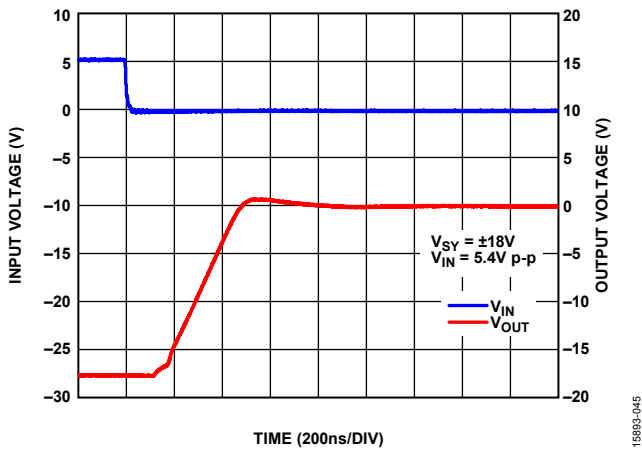


Figure 49. Negative Overload Recovery, $A_V = -10$, $V_{SY} = \pm 18\text{ V}$

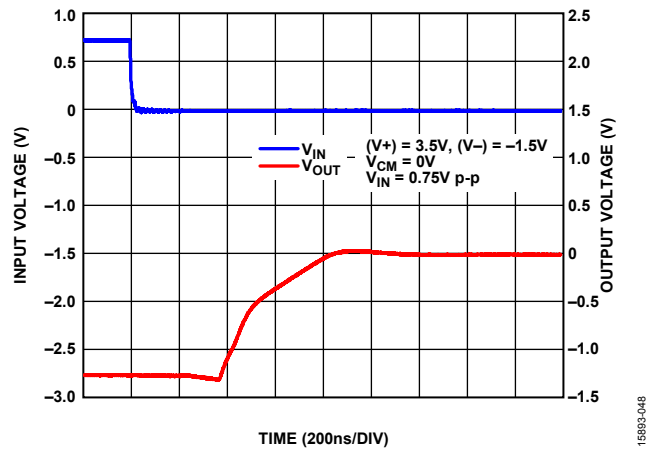


Figure 52. Negative Overload Recovery, $A_V = -10$, $V_{SY} = 5\text{ V}$

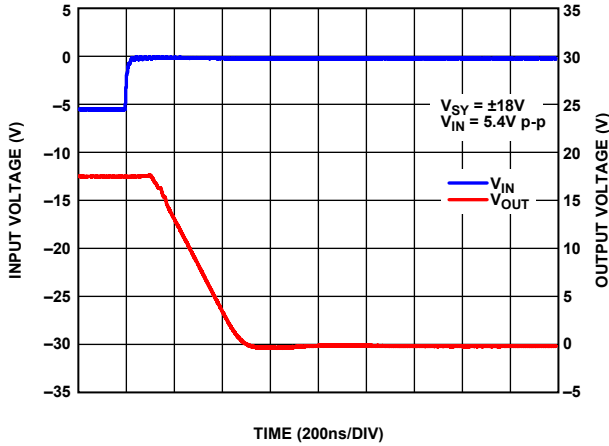


Figure 53. Positive Overload Recovery, $A_v = -10$, $V_{SY} = \pm 18 V$

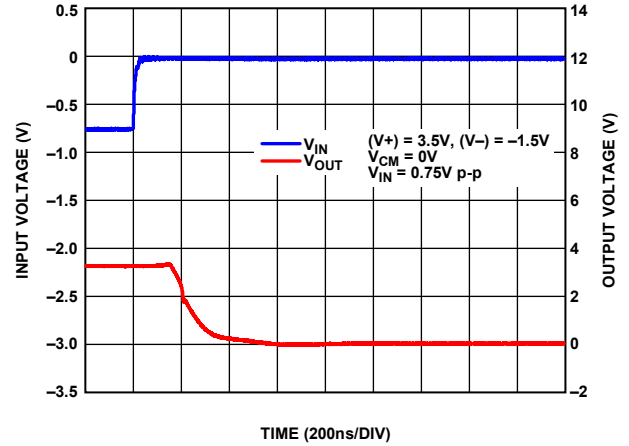


Figure 56. Positive Overload Recovery, $A_v = -10$, $V_{SY} = 5 V$

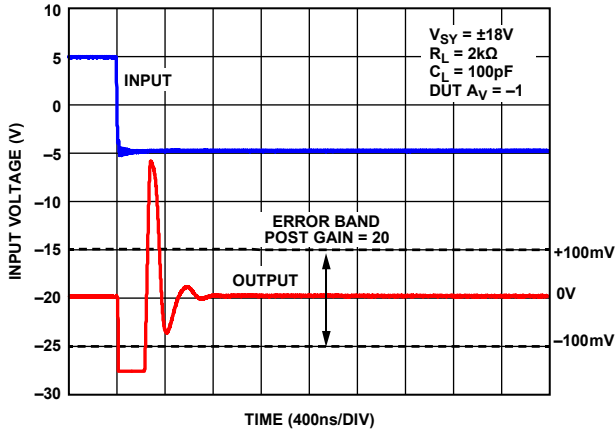


Figure 54. ADA4625-1 Negative Settling Time to 0.1%, $V_{SY} = \pm 18 V$

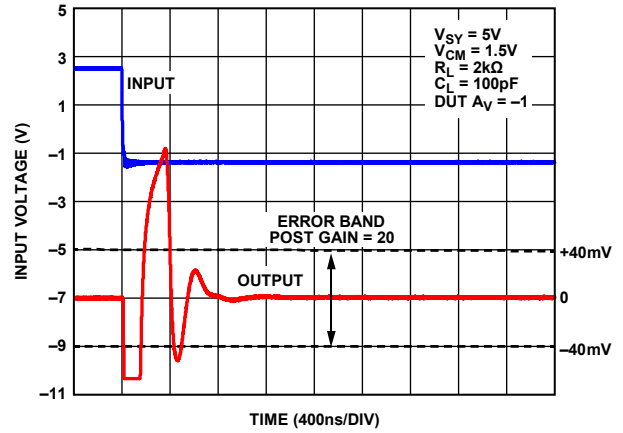


Figure 57. ADA4625-1 Negative Settling Time to 0.1%, $V_{SY} = 5 V$

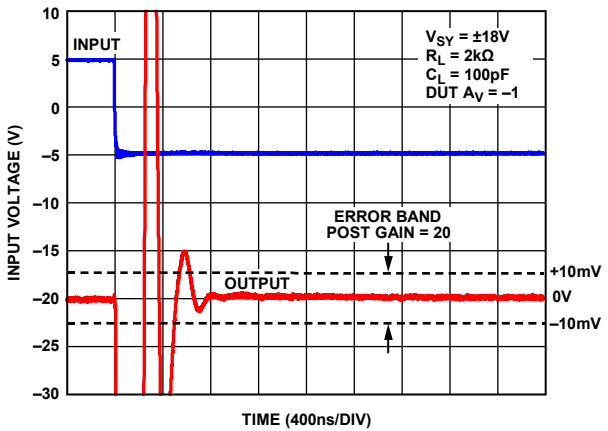


Figure 55. ADA4625-1 Negative Settling Time to 0.01%, $V_{SY} = \pm 18 V$

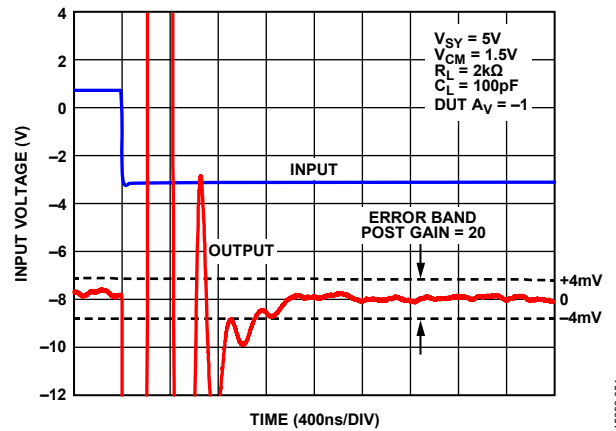


Figure 58. ADA4625-1 Negative Settling Time to 0.01%, $V_{SY} = 5 V$

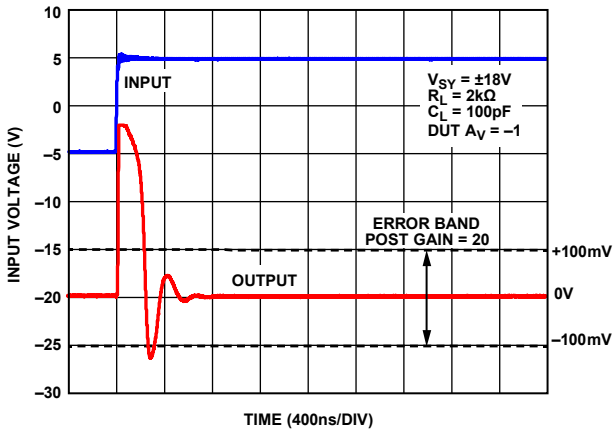


Figure 59. ADA4625-1 Positive Settling Time to 0.1%, $V_{SY} = \pm 18V$

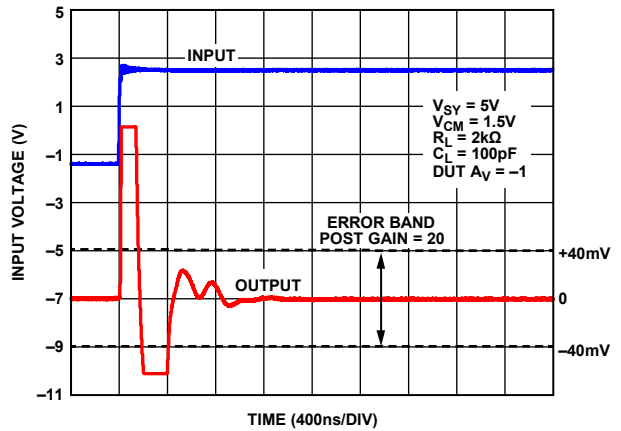


Figure 62. ADA4625-1 Positive Settling Time to 0.1%, $V_{SY} = 5V$

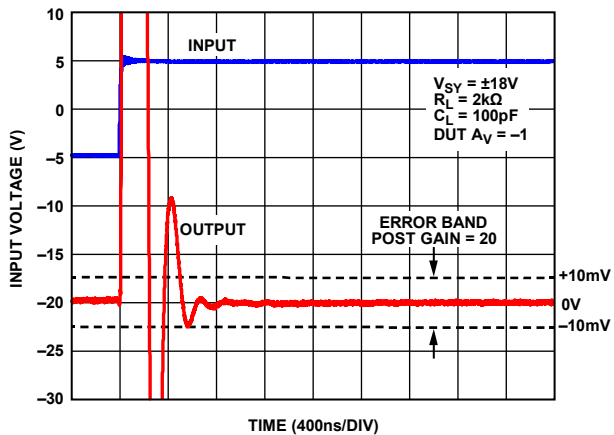


Figure 60. ADA4625-1 Positive Settling Time to 0.01%, $V_{SY} = \pm 18V$

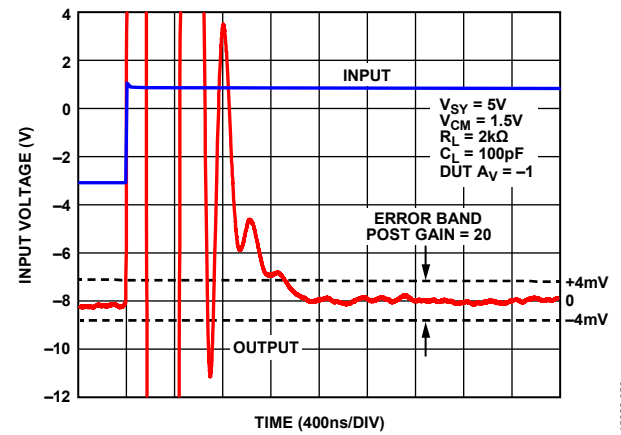


Figure 63. ADA4625-1 Positive Settling Time to 0.01%, $V_{SY} = 5V$

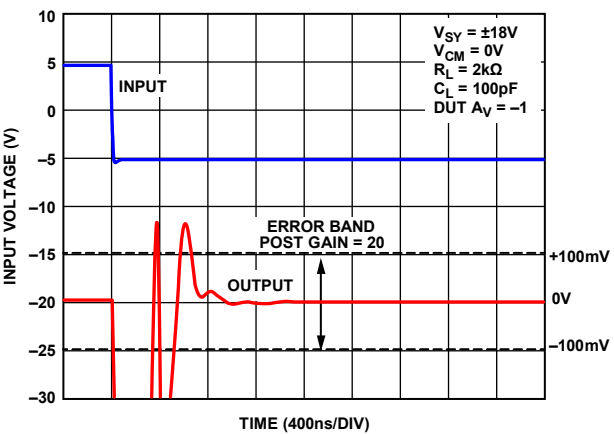


Figure 61. ADA4625-2 Negative Settling Time to 0.1%, $V_{SY} = \pm 18V$

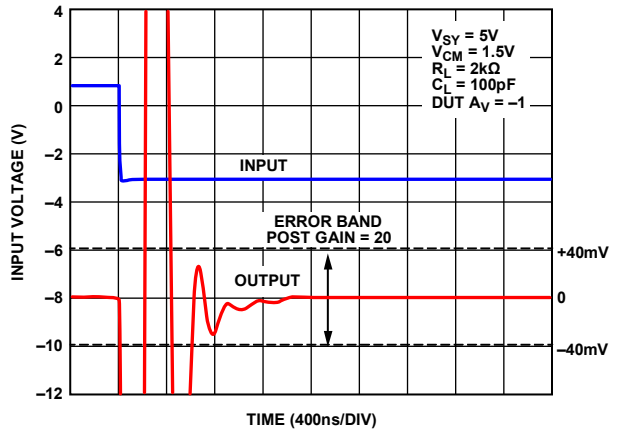


Figure 64. ADA4625-2 Negative Settling Time to 0.1%, $V_{SY} = 5V$

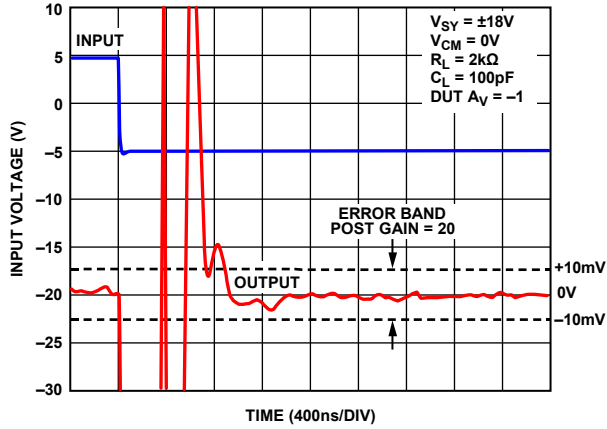


Figure 65. ADA4625-2 Negative Settling Time to 0.01%, $V_{SY} = \pm 18V$

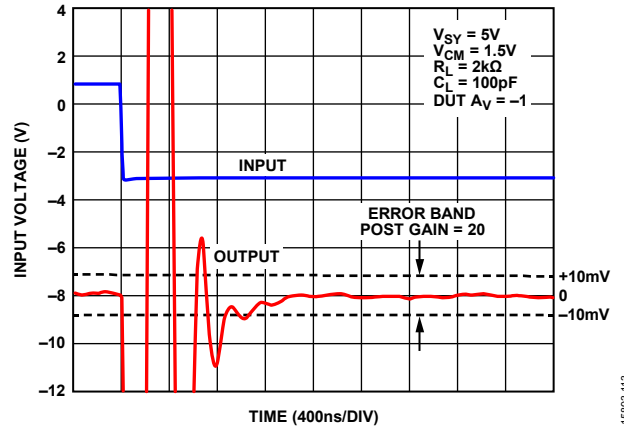


Figure 68. ADA4625-2 Negative Settling Time to 0.01%, $V_{SY} = 5V$

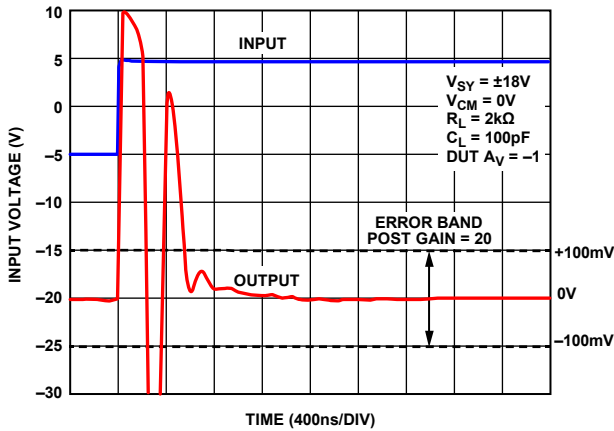


Figure 66. ADA4625-2 Positive Settling Time to 0.1%, $V_{SY} = \pm 18V$

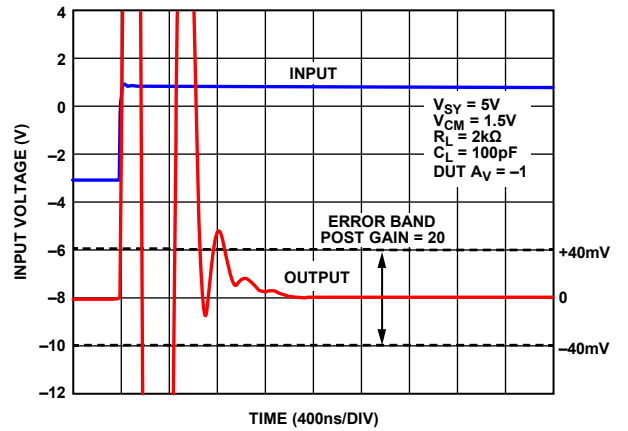


Figure 69. ADA4625-2 Positive Settling Time to 0.1%, $V_{SY} = 5V$

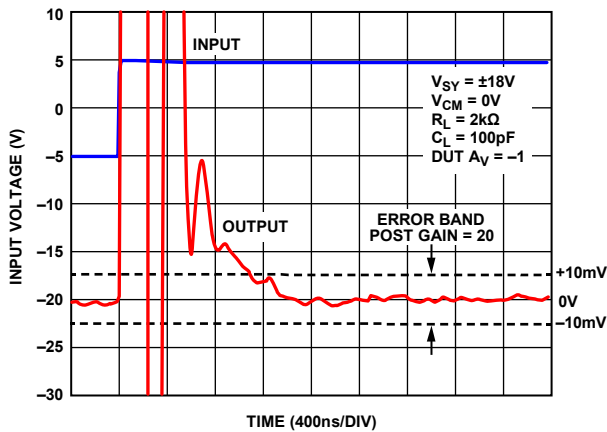


Figure 67. ADA4625-2 Positive Settling Time to 0.01%, $V_{SY} = \pm 18V$

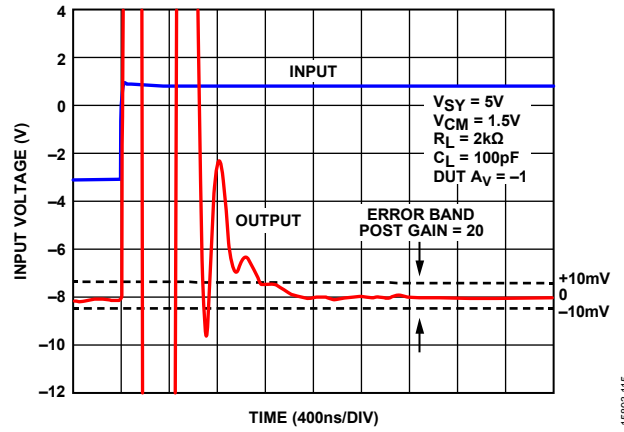


Figure 70. ADA4625-2 Positive Settling Time to 0.01%, $V_{SY} = 5V$

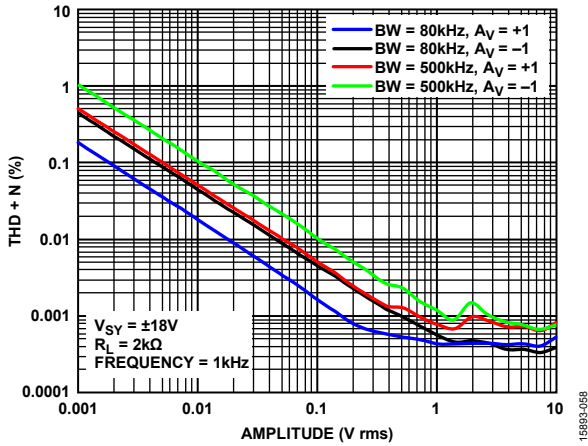


Figure 71. ADA4625-1 Total Harmonic Distortion + Noise (THD + N) vs. Amplitude, $V_{SY} = \pm 18V$ (BW Means Bandwidth)

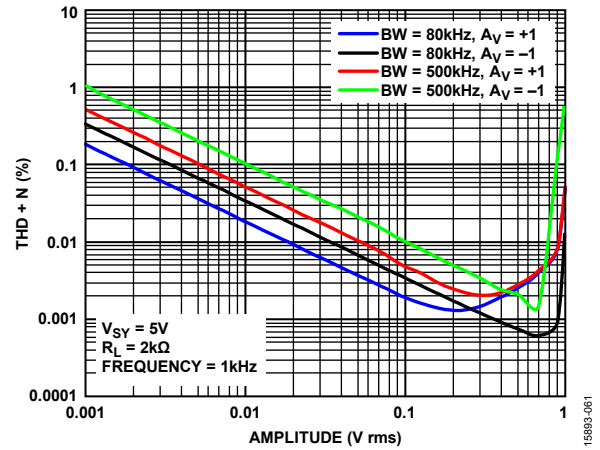


Figure 74. ADA4625-1 THD + N vs. Amplitude, $V_{SY} = 5V$

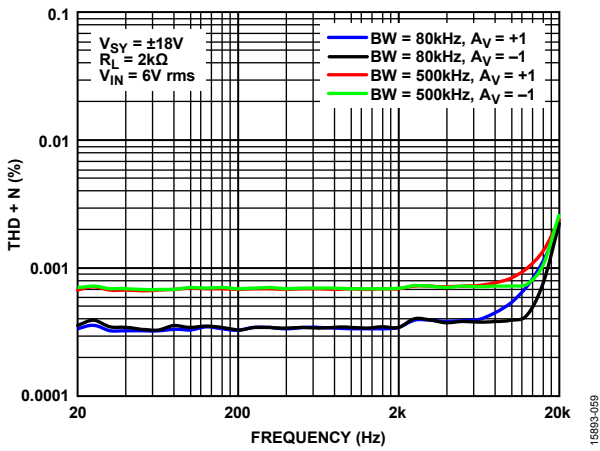


Figure 72. ADA4625-1 THD + N vs. Frequency, $V_{SY} = \pm 18V$

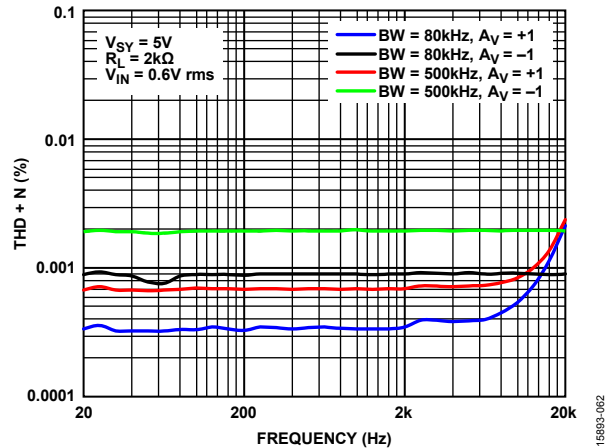


Figure 75. ADA4625-1 THD + N vs. Frequency, $V_{SY} = 5V$

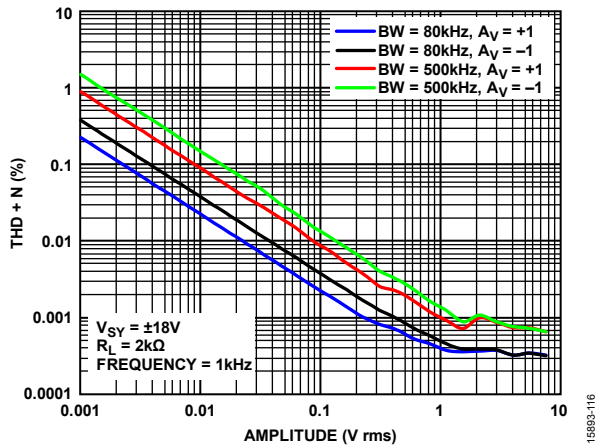


Figure 73. ADA4625-2 THD + N vs. Amplitude, $V_{SY} = \pm 18V$

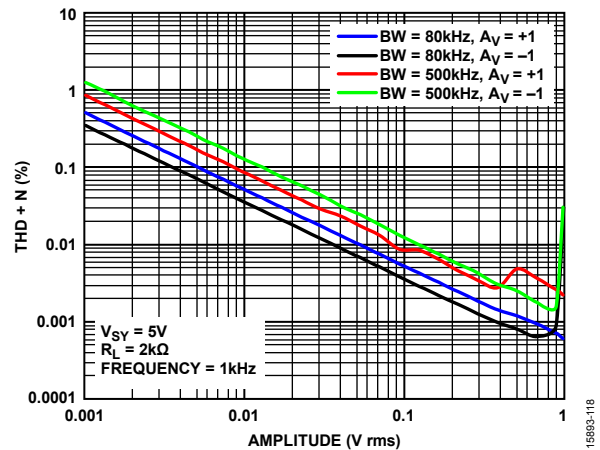


Figure 76. ADA4625-2 THD + N vs. Amplitude, $V_{SY} = 5V$

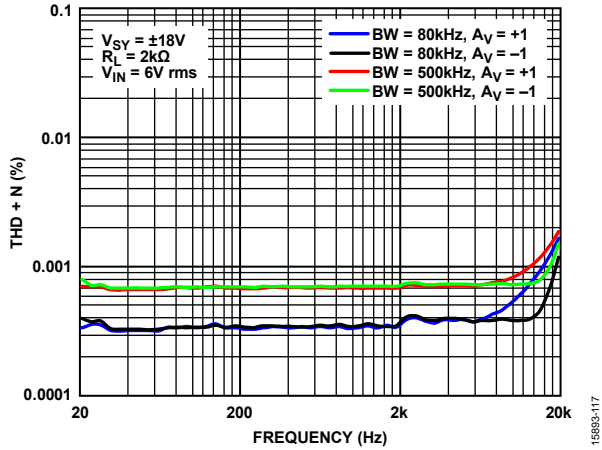


Figure 77. ADA4625-2 THD + N vs. Frequency, $V_{SY} = \pm 18V$

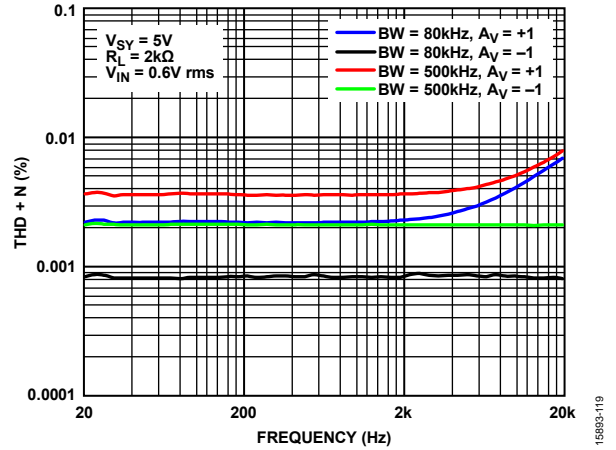


Figure 80. ADA4625-2 THD + N vs. Frequency, $V_{SY} = 5V$

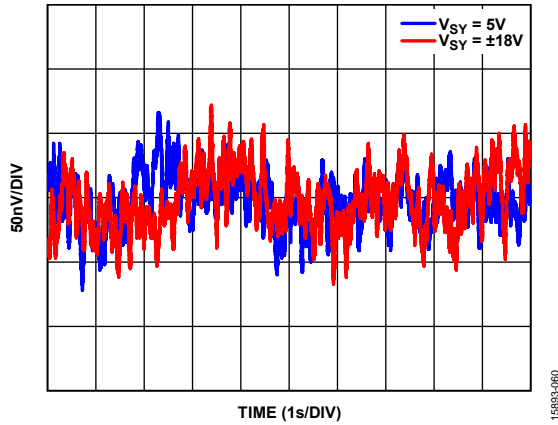


Figure 78. 0.1 Hz to 10 Hz Noise

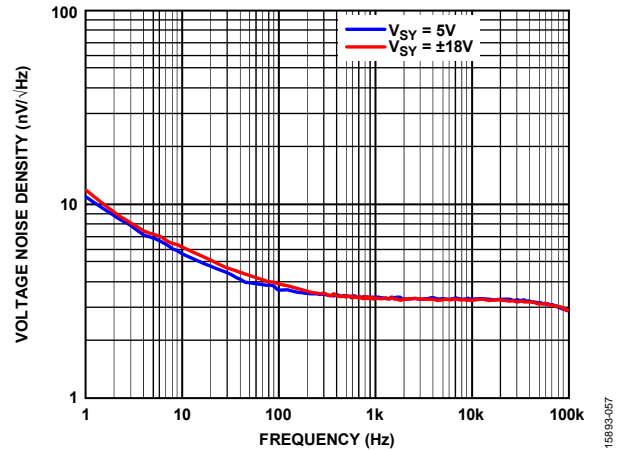


Figure 81. Voltage Noise Density vs. Frequency

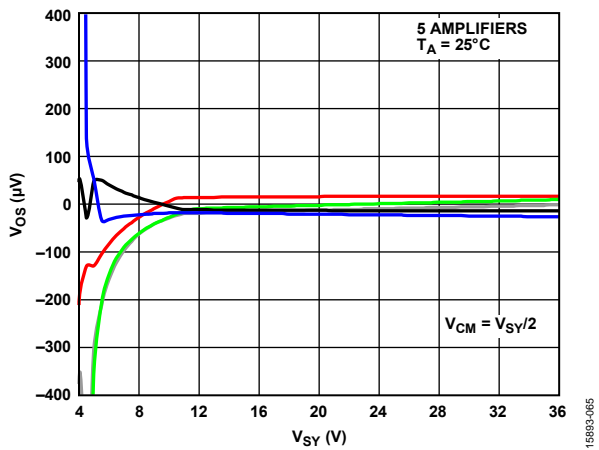


Figure 79. V_{OS} vs. V_{SY}

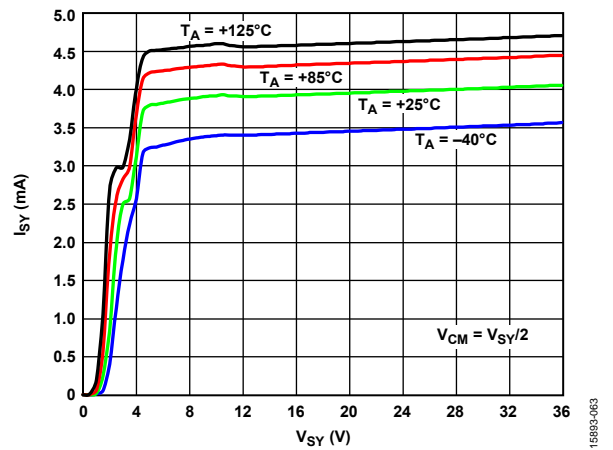


Figure 82. Supply Current (I_{SV}) vs. V_{SY} for Various Temperatures

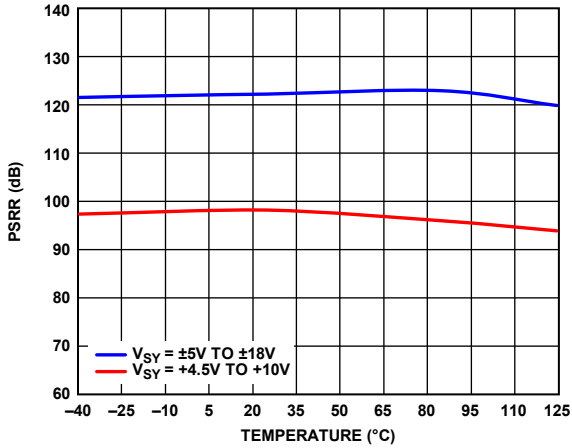


Figure 83. PSRR vs. Temperature

15893-032

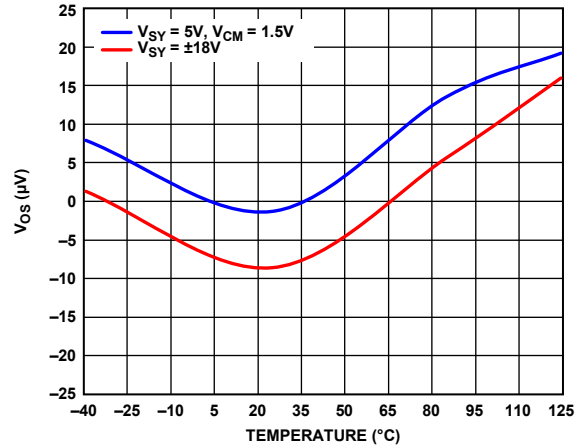


Figure 85. Vos vs. Temperature

15893-009

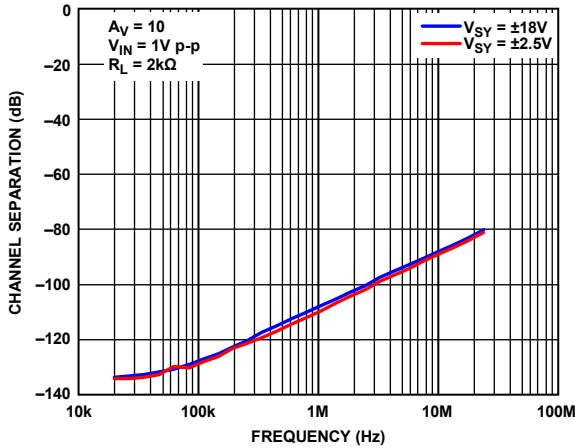


Figure 84. Channel Separation vs. Frequency

15893-120

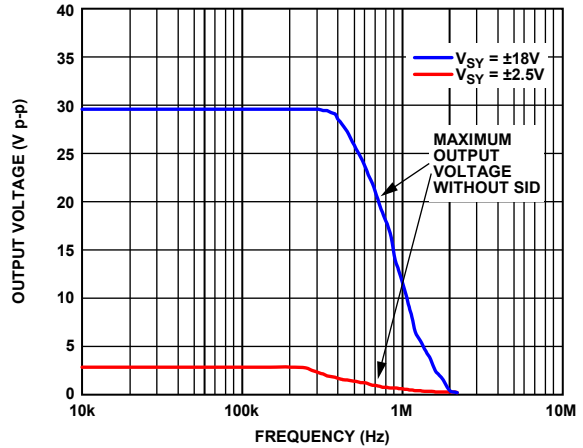


Figure 86. Maximum Peak-to-Peak Output Voltage Without Slew Rate Induced Distortion (SID) vs. Frequency

15893-064

THEORY OF OPERATION

Figure 87 shows the simplified circuit diagram for the ADA4625-1/ADA4625-2. The JFET input stage architecture offers the advantages of low input bias current, high bandwidth, high gain, low noise, and no phase reversal when the applied input signal exceeds the common-mode voltage range. The output stage is rail to rail with high drive characteristics and low dropout voltage for both sinking and sourcing currents.

INPUT AND GAIN STAGES

To achieve high input impedance, low noise, low offset, and low offset drift, the ADA4625-1/ADA4625-2A uses large input N channel JFETs (M1 and M2). These JFETs operate with the S source at about 1.2 V above the G gate. In the worst case, the source is only 0.9 V above the gate. By design, the normal operation of the input tail current (I_{TAIL}) extends down to 0.6 V above V_- , which gives the ADA4625-1/ADA4625-2 an input common-mode range down to 0.2 V below V_- with margin. Resistive loads keep the noise low. The BUFF1 buffer drives the top of the input load resistors (R1 and R2), keeping the voltage drop across M1 and M2 nearly constant, making a virtual cascode. The differences

of the input voltages of +IN and -IN steer I_{TAIL} through M1 and M2 to R1 and R2, generating a differential voltage. The first voltage to current gain block (GM1) translates that differential voltage into differential currents (I_1 and I_2) that drive the current mirror (Q1 and Q2), which generates a differential voltage between the reference node and gain node. JFET inputs of the second voltage to current gain block (GM2) maximizes the gain node impedance, giving the ADA4625-1/ADA4625-2 a high gain.

OUTPUT STAGE

The GM2 gain block generates two pairs of differential currents. One pair drives the bottom current mirror (Q3 and Q4) and the NPN output transistor (Q7), and the second pair drives the top current mirror (Q5 and Q6) and the output PNP transistor (Q8). The common emitter output transistors (Q7 and Q8) source and sink current rail to rail. GM2 also senses the base voltages of Q7 and Q8 and adjusts the I_4 and I_6 currents; with no output load, Q7 and Q8 collector currents are 0.6 mA. In addition, GM2 clamps the base voltages of Q7 and Q8 so neither completely turns off.

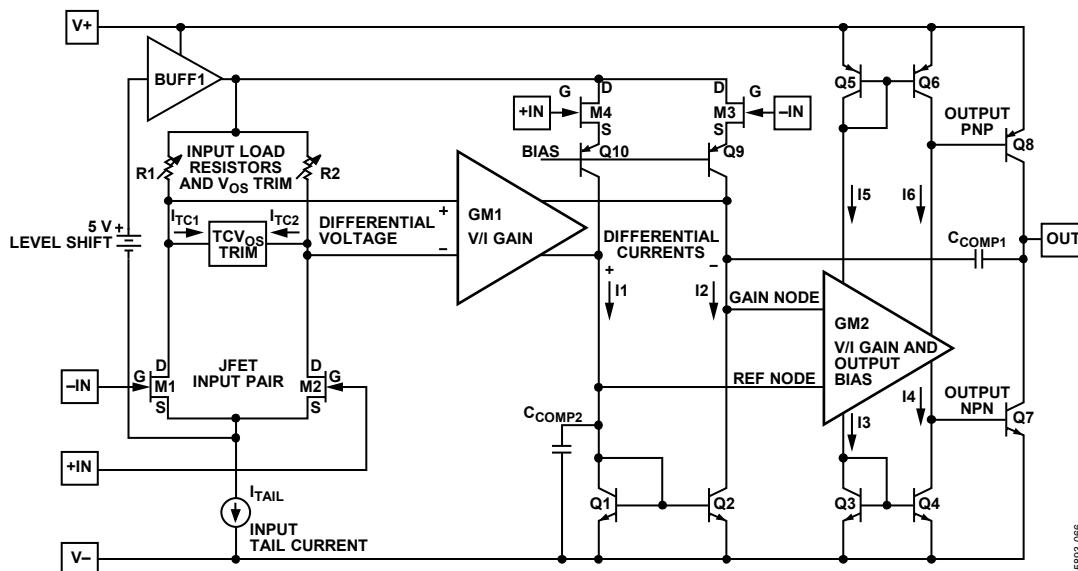


Figure 87. Simplified Circuit Diagram

15893-066

NO PHASE INVERSION

Rail-to-rail output (RRO) amplifiers without rail-to-rail input (RRI) are prone to phase inversion because the output can drive the input outside of the normal common-mode range, causing the output to go in the wrong direction and latch up. To prevent phase inversion, the input must control the input at all times. Even though the RRO of the ADA4625-1/ADA4625-2 input stage (M1, M2, R1, and R2) operates correctly down to 0.2 V below V^- , it does not operate correctly within 2.5 V of V^+ . The ADA4625-1/ADA4625-2 guarantees no phase inversion by implementing an input pair (M3 and M4) to extend the common-mode range to 0.2 V above V^+ , with reduced performance. M3 and M4 are not active in the normal common-mode range. Figure 88 shows that the input voltage exceeds both supplies by 200 mV with no phase inversion at the output.

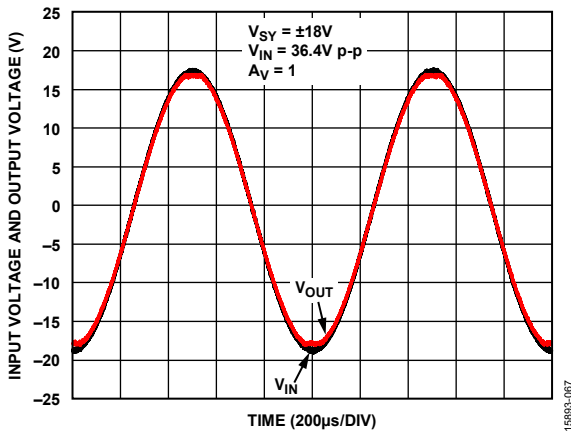


Figure 88. No Phase Reversal if the Input Range Exceeds the Power Supply by 200 mV

SUPPLY CURRENT

The supply current (I_{SY}) is the quiescent current drawn by the op amp with no load. Figure 89 and Figure 90 show that the quiescent current varies with the common-mode input voltage. The shape of I_{SY} vs. V_{CM} at higher V_{CM} shows saturation of BUFF1 and the I_{TAIL} turn off.

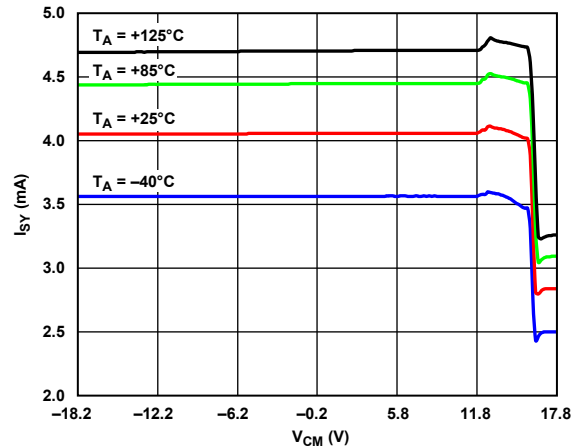


Figure 89. I_{SY} vs. V_{CM} , $V_{SY} = \pm 18 V$

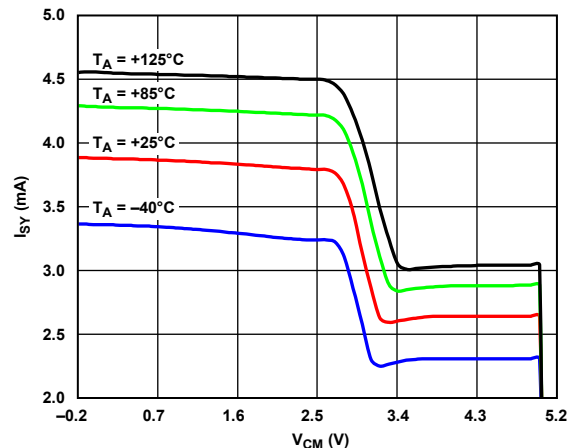


Figure 90. I_{SY} vs. V_{CM} , $V_{SY} = 5 V$

APPLICATIONS INFORMATION

ACTIVE LOOP FILTER FOR PHASE-LOCKED LOOPS (PLLs)

PLL Basic

A PLL is a feedback system that combines a phase detector (PD), a loop filter, and a voltage controlled oscillator (VCO) that is so connected that the oscillator maintains a constant frequency (or phase angle) relative to the reference signal. The functional block diagram of a basic PLL is shown in Figure 91.

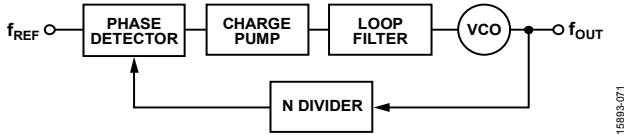


Figure 91. Basic PLL

The phase detector detects the phase difference between the input reference signal and the feedback signal. The resulting error signal is proportional to the relative phase of the input and the feedback signals. The charge pump converts the PD error signal into current pulses. A loop filter circuit is typically required to integrate and smooth the source and sink current pulses from the charge pump into a voltage, which in turn drives the VCO. The VCO outputs a range of frequencies depending on the voltage level at its tuning port. By making the frequency N divider programmable, the VCO frequency can be tuned in either integer steps or fractional amounts characterizing the PLL as either an integer-N PLL or a fractional-N PLL. Because a PLL is a negative feedback loop, the output of the VCO adjusts as necessary until the frequency error signal is zero and the PLL is in lock. The output frequency is given by $f_{OUT} = N \times f_{REF}$.

Figure 92 shows the block diagram of the basic PLL model in the Laplace transform format, where f_{REF} is the frequency of the input signal, and f_{OUT} is the frequency of the VCO output signal. Because the phase difference is the integral of the frequency difference, there is a $1/s$ term in the PLL loop.

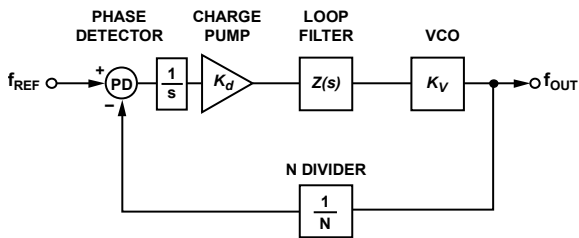


Figure 92. Basic PLL Model

Loop Filter

The loop filter, which smooths out the error signal, is a critical part of the system. For applications that require low phase noise and a wide tuning range, design the VCO with a low gain and a large input voltage range to satisfy these requirements. When the required VCO tuning voltage is higher than the maximum voltage the charge pump can supply, implement an active loop filter comprising of an op amp with gain to accommodate the higher tuning voltages. Figure 93 and Figure 94 illustrate the typical active loop filters in inverting and noninverting topologies, respectively, with prefiltering.

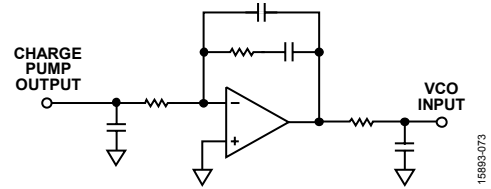


Figure 93. Typical Active Loop Filter—Inverting Topology

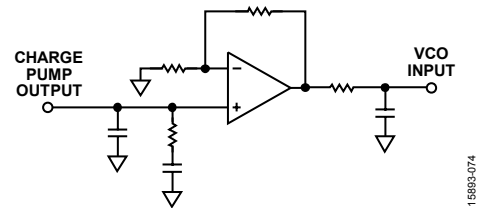


Figure 94. Typical Active Loop Filter—Noninverting Topology

The inverting topology has the advantage of biasing the charge pump output at a fixed voltage, typically one-half the charge pump voltage ($V_P/2$), which is optimal for spur performance. When using the inverting topology, ensure that the PLL IC allows the phase detector polarity to be inverted for the correct polarity voltage at the output of the op amp for driving the VCO.

ADA4625-1 ADVANTAGES AND DESIGN EXAMPLE

The op amp choice for an active filter affects the key performance parameters of the PLLs: frequency range, phase noise, spurious frequencies, and lock time. The output of the filter directly affects the generated frequency and phase. Low noise is essential because any voltage noise applied to the tuning port of the VCO is amplified by the VCO gain and translated into phase noise. Low input bias current is also recommended because the op amp bias current must be sourced from the PLL phase detector/ charge pump, and any mismatch or leakage at the output of the phase detector between the up and down currents causes ripples and reference spurs.

With 18 MHz gain bandwidth product (GBP), low input bias currents (± 15 pA), low voltage noise density (3.3 nV/ $\sqrt{\text{Hz}}$), ultralow current noise density, and low 1/f corner frequency, the ADA4625-1 is an ideal op amp for using in a PLL active loop filter. The ADA4625-1 does not require a negative voltage supply because of its ground sensing input. The rail-to-rail output stage is beneficial in terms of increasing the flexibility in biasing the op amp so that the output range of the PLL is mapped efficiently onto the input range of the VCO. In addition, the wide 5 V to 36 V operating supply range makes the ADA4625-1 a versatile choice for the design of a wide variety of active loop filters.

Figure 96 shows the ADA4625-1 as the loop filter for the ADF4159, a 13 GHz fractional-N synthesizer. The phase detector polarity of the ADF4159 is programmed to negative because the ADA4625-1 is used in an inverting active loop filter

configuration. The VCO is set up to feedback the VCO/2 output to the ADF4159. The loop filter has a 900 kHz loop bandwidth (LBW) and a phase margin of 58° with 2.5 mA charge pump current. Lowering the bandwidth further improves phase noise at the expense of increased PLL lock time.

Figure 95 shows the PLL loop filter transfer function. Capacitor C1 and Resistor R1 change the phase detector current pulses into a continuous time voltage waveform. At frequencies lower than the R2C2 zero, the amplifier and R1C2 form an integrator. Between the R2C2 zero and the R2C3 pole, the gain is constant at the value set by R2/R1. Above the R2C3 pole, the amplifier is an integrator until R1C3 becomes a feedforward noninverting zero path around the amplifier. Resistor R3 and Capacitor C4 add an additional pole in the loop filter signal path. Setting the R3C4 pole below the R2C3 pole reduces the effect of the R1C3 feedforward zero.

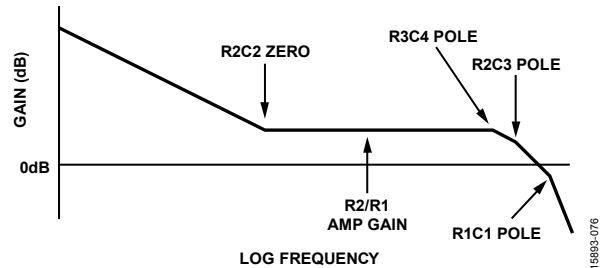


Figure 95. PLL Loop Filter Transfer Function

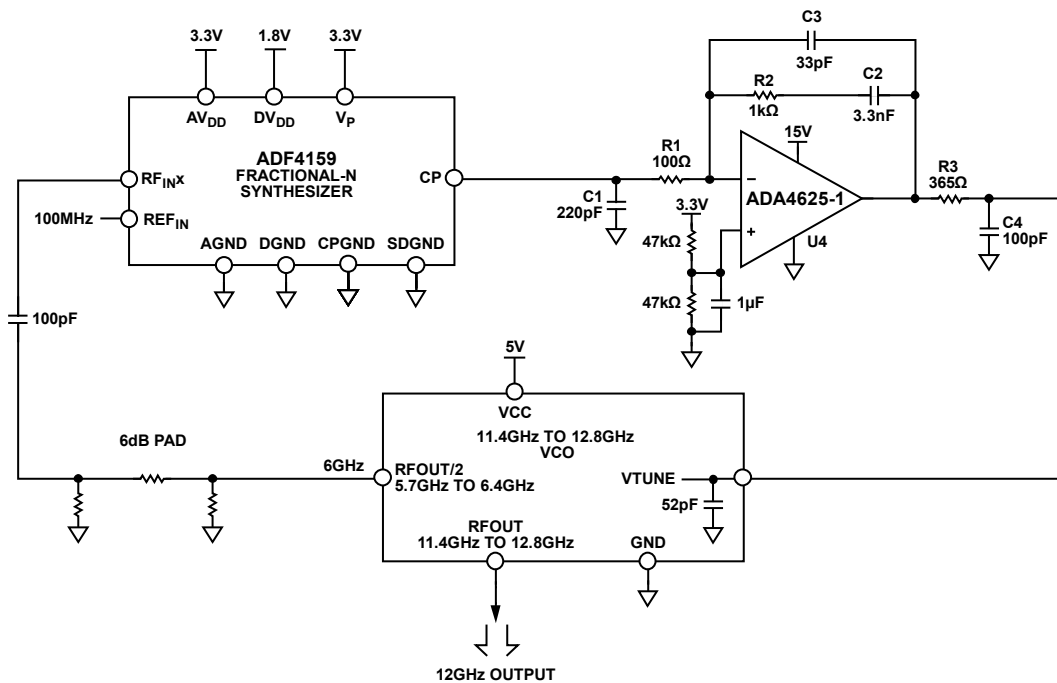


Figure 96. Block Diagram of ADA4625-1 Active Loop Filter for ADF4159

PLLs in which the loop gain passes through 0 dB above the R2C2 zero and below the R2C3 pole and R3C4 pole are stable. At low charge pump currents, the loop gain passes through zero above R2C2 zero. At high charge pump currents, the loop gain passes through zero below the R2C3 pole and R3C4 pole (see Figure 97).

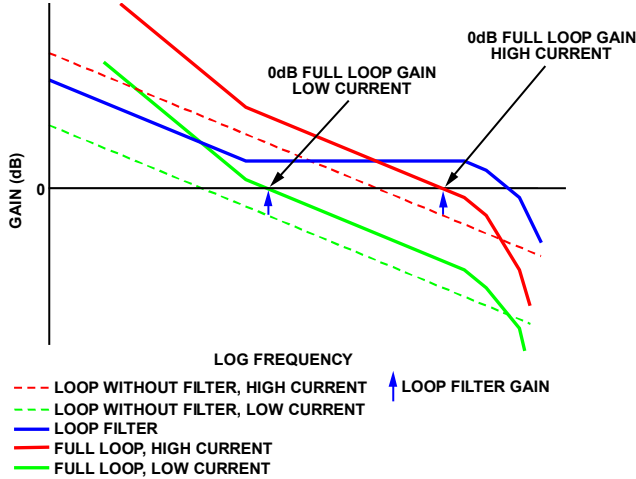


Figure 97. Gain vs. Frequency of PLL and Loop Filter

Figure 98 shows the measured phase noise vs. frequency offset from 12 GHz carrier for different charge pump currents (I_{CP}). Generally, most operations have a charge pump current of 2.5 mA and below. Refer to the [UG-383 User Guide](#) for details on running these tests and setting up the software required.

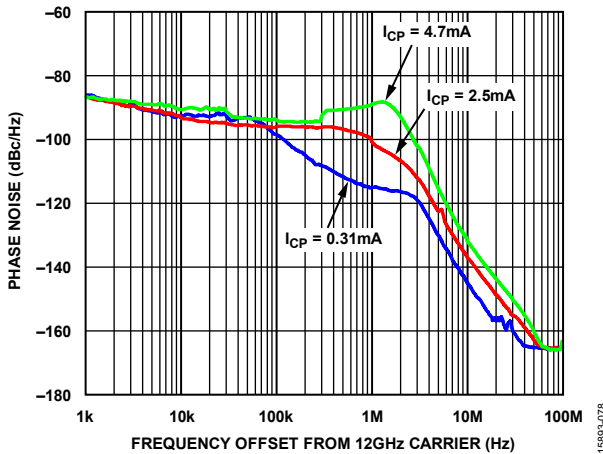


Figure 98. Phase Noise vs. Frequency Offset from 12 GHz Carrier for Different Charge Pump Currents (I_{CP})

The Analog Devices simulation tool, [ADIsimPLL](#), allows the design and simulation of PLL loop filter topologies and has a library of Analog Devices op amps built in. The simulation tool accurately predicts PLL closed-loop phase noise and is able to model the effect of op amp noise along with the noise of the other PLL loop components. For more information about the [ADIsimPLL](#) design tools, refer to www.analog.com/ADIsimPLL.

TRANSIMPEDANCE AMPLIFIER

The ADA4625-1 is an excellent choice for low noise transimpedance amplifier (TIA) applications. While its low voltage and current noise maximize signal-to-noise ratio (SNR), its low voltage offset and input bias current minimize the dc error at the amplifier output. Having a true ground sense capability, the ADA4625-1 is ideal for single-supply operation. In addition, its rail-to-rail output swing allows the detection and amplification of a wide range of input current signals. Figure 99 shows the ADA4625-1 as a current to voltage (I-V) converter with an electrical model of a photodiode.

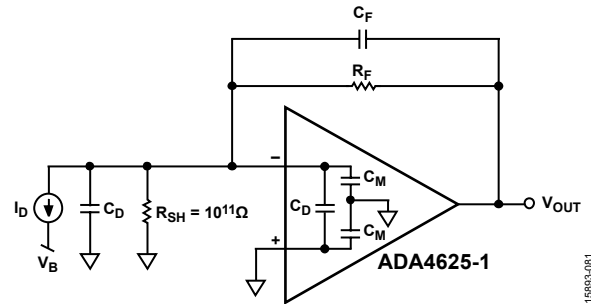


Figure 99. Equivalent TIA Circuit

Photodiodes can operate in either photovoltaic mode (zero bias) or photoconductive mode (with an applied reverse-bias across the diode). Mode selection depends on the speed and dark current requirements of the application and the choice of photodiode. In photovoltaic mode, the dark current is at a minimum and is preferred for low frequency and/or low light level applications (that is, PN photodiodes). Photoconductive mode is better for applications that required faster and linear responses (that is, PIN photodiodes); however, the tradeoffs include increases in dark and noise currents.

The following transfer function describes the transimpedance gain of Figure 99:

$$V_{OUT} = \frac{I_D R_F}{1 + s C_F R_F} \tag{1}$$

where:

V_{OUT} is the desired output dc voltage of the op amp.

I_D is the output current of the photodiode.

R_F and C_F are the feedback resistor and capacitor. The parallel combination of R_F and C_F sets the signal bandwidth.

s is the s plane.

Set R_F such that the maximum attainable output voltage corresponds to the maximum diode output current. Because signal levels increase directly with R_F , while the noise due to R_F increases with the square root of the resistor value, employing the full output swing maximizes the SNR.

It is important to distinguish between the signal gain and the noise gain (NG) because the noise gain characteristics determine the net circuit stability. The noise gain has the same transfer function as the noninverting signal gain, which follows:

$$NG = \left(1 + \frac{R_F}{R_{SH}}\right) \times \frac{1 + s(R_F // R_{SH})(C_{IN} + C_F)}{1 + sR_F C_F} \quad (2)$$

where:

R_{SH} is the diode shunt resistance.

C_{IN} is the total input capacitance consisting of the sum of the diode shunt capacitance (C_D), the input capacitance of the amplifier ($C_{DM} + C_{CM}$), and the external stray capacitance.

C_{IN} and R_F produce a zero in the noise gain transfer function and the zero frequency (f_Z) is as follows:

$$f_Z = \frac{1}{2\pi(R_F // R_{SH})(C_{IN} + C_F)} \quad (3)$$

Because the photodiode shunt resistance $R_{SH} \gg R_F$, the circuit behavior is not impacted by the effect of the junction resistance, and f_Z simplifies to

$$f_Z = \frac{1}{2\pi R_F (C_{IN} + C_F)} \quad (4)$$

Figure 100 shows the TIA noise gain superimposed upon the open loop gain of the amplifier. For the system to be stable, the noise gain curve must intersect with the open loop response with a net slope of less than 20 dB/decade. In Figure 100, the dotted line shows an uncompensated noise gain ($C_F = 0$ pF) intersecting with the open loop gain at the frequency (f_X) with a slope of 20 dB/decade, indicating an unstable condition.

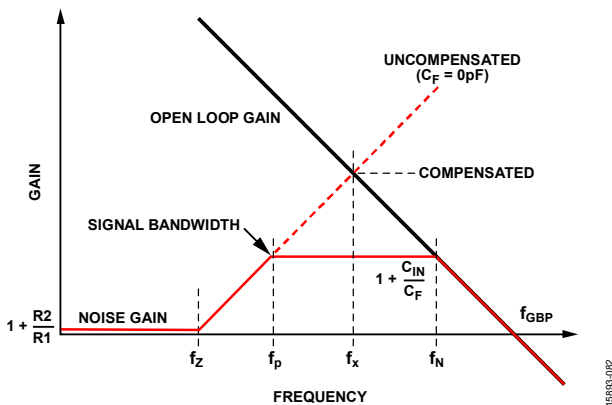


Figure 100. Generalized TIA Noise Gain and Transfer Function

The instability caused by C_{IN} can be compensated by adding C_F to introduce a pole at a frequency equal to or lower than f_X . The pole frequency is as follows:

$$f_P = \frac{1}{2\pi R_F C_F} \quad (5)$$

Setting the pole at the f_X frequency maximizes the signal bandwidth with a 45° phase margin but is marginal for stability, as indicated by the dashed line. Because f_X is the geometric mean of f_Z and the gain bandwidth product frequency (f_{GBP}) of the amplifier, calculate f_X by

$$f_X = \sqrt{f_Z f_{GBP}} \quad (6)$$

Substituting Equation 4 and Equation 5 into Equation 6, the C_F value that produces f_X is

$$C_F = \frac{1 + \sqrt{1 + 8\pi R_F C_{IN} f_{GBP}}}{4\pi R_F f_{GBP}} \quad (7)$$

If $8\pi \times R_F \times C_{IN} \times f_{GBP} \gg 1$, Equation 7 simplifies to

$$C_F = \sqrt{\frac{C_{IN}}{2\pi R_F f_{GBP}}} \quad (8)$$

Adding C_F also sets the signal bandwidth at f_P . Substitute Equation 8 into Equation 5 and rearrange the equation for the signal bandwidth in terms of f_{GBP} , R_F , and C_{IN} :

$$f_P = \sqrt{\frac{f_{GBP}}{2\pi R_F C_{IN}}} \quad (9)$$

Notice the attainable signal bandwidth is a function of the time constant $R_F C_{IN}$ and the f_{GBP} of the amplifier. To maximize the signal bandwidth, choose an op amp with high bandwidth and low input capacitance, and operate the photodiode in reverse bias to reduce its junction capacitance.

Because the input current noise of the FET input op amp is negligible, and the shot noise of the photodiode is negligible due to the filtering effect of the shunt capacitance, the dominant sources of output noise in the wideband photodiode TIA circuit are the input voltage noise of the amplifier e_N and the thermal noise generated by R_F .

At low frequencies, the circuit noise gain is $1 + R_F/R_{SH}$. At frequencies equal to or greater than f_Z , the noise gain begins to increase and plateau when the gain is $1 + C_{IN}/C_F$ (see Figure 100). In addition, the noise bandwidth frequency, f_N (where the compensated noise gain intersecting the open loop gain), can be estimated by

$$f_N = \frac{C_F}{(C_{IN} + C_F)} f_{GBP} \quad (10)$$

Design Example

As a design example, Figure 101 shows the ADA4625-1 configured as a TIA amplifier in a photodiode preamp application. Assuming the photodiode has a C_D of 5 pF and an I_D of 200 μ A, and the desired full-scale V_{OUT} is 10 V, and using Equation 1, R_F is 50 k Ω .

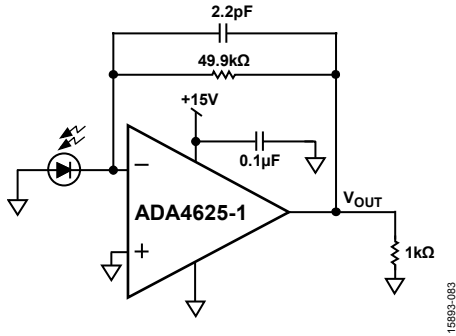


Figure 101. Single-Supply TIA Circuit Using the ADA4625-1

The ADA4625-1 input capacitance ($C_{CM} + C_{DM}$) is 19.9 pF; therefore, the total input capacitance (C_{IN}) is 24.9 pF. By substituting $C_{IN} = 24.9$ pF, $R_F = 50$ k Ω , and $f_{GBP} = 18$ MHz into Equation 7 and Equation 9, the resulting feedback capacitor value (C_F) and the -3 dB signal bandwidth (f_P) are 2.2 pF and 1.45 MHz, respectively.

Figure 102 and Figure 103 show the compensations of the TIA circuit. The system has a bandwidth of 1.45 MHz when it is maximized for a signal bandwidth with $C_F = 2.2$ pF. Increasing C_F to 3.9 pF reduces the bandwidth to 0.82 MHz; however, it greatly reduces the overshoot (see Figure 104). In practice, an optimum C_F value is determined experimentally by varying it slightly to optimize the output pulse response.

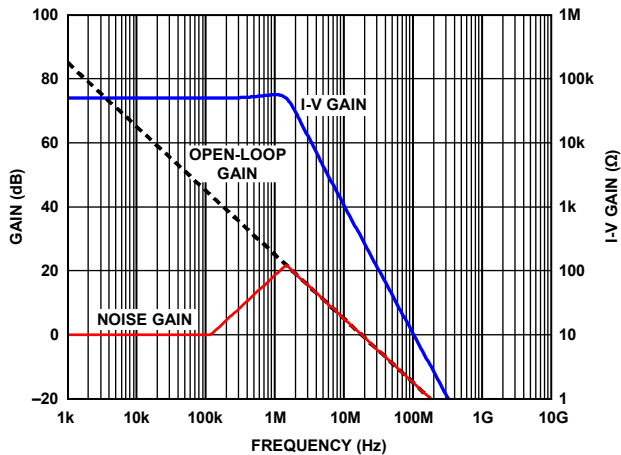


Figure 102. Compensating the TIA, $C_F = 2.2$ pF

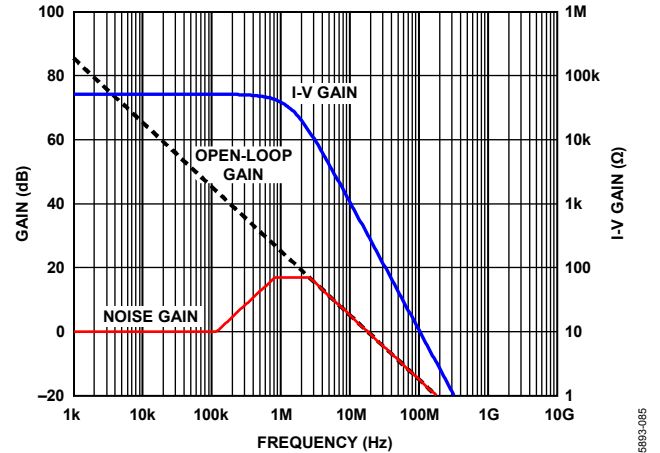


Figure 103. Compensating the TIA, $C_F = 3.9$ pF

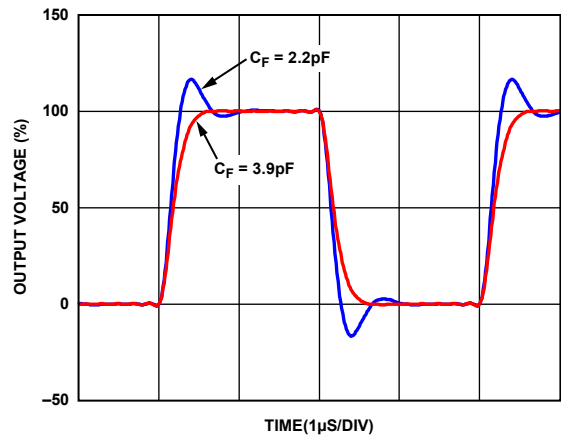


Figure 104. Pulse Response vs. C_F

Table 8 shows the noise sources and estimated total output noise for the photodiode amplifier with $C_F = 2.2 \text{ pF}$ and $C_F = 3.9 \text{ pF}$, respectively.

Use the Analog Devices [Analog Photodiode Wizard](#) to design a transimpedance amplifier circuit to interface with a photodiode.

Table 8. RMS Noise Contributions of the Photodiode Preamplifier

Noise Contributor	Expression	RMS Noise (μV) ¹	
		$C_F = 2.2 \text{ pF}$	$C_F = 3.9 \text{ pF}$
R_F	$\sqrt{4kTR_F \left(\frac{\pi}{2} f_p\right)}$ where: k is Boltzmann's constant ($1.38 \times 10^{-23} \text{ J/K}$). T is the temperature in Kelvin (K).	43.2	32.5
Current Noise, $V_{ni, AMP}$	$i_N R_F \sqrt{\frac{\pi}{2} f_p}$	0.34	0.25
Voltage Noise, $V_{nv, AMP}$	$e_N \sqrt{\left(1 + \frac{C_{IN}}{C_F}\right) \frac{\pi}{2} f_{GBP}}$	61.6	47.7
Total Noise	$\sqrt{V_{nv, AMP}^2 + V_{ni, AMP}^2 + V_{R_f}^2}$	75.2	57.7

¹ RMS noise with $R_F = 49.9 \text{ k}\Omega$, $C_{IN} = C_{CM} + C_{DM} = 19.9 \text{ pF}$, $C_D = 5 \text{ pF}$, $i_n = 4.5 \text{ fA}/\sqrt{\text{Hz}}$, and $e_n = 3.3 \text{ nV}/\sqrt{\text{Hz}}$.

DAC OUTPUT DRIVER

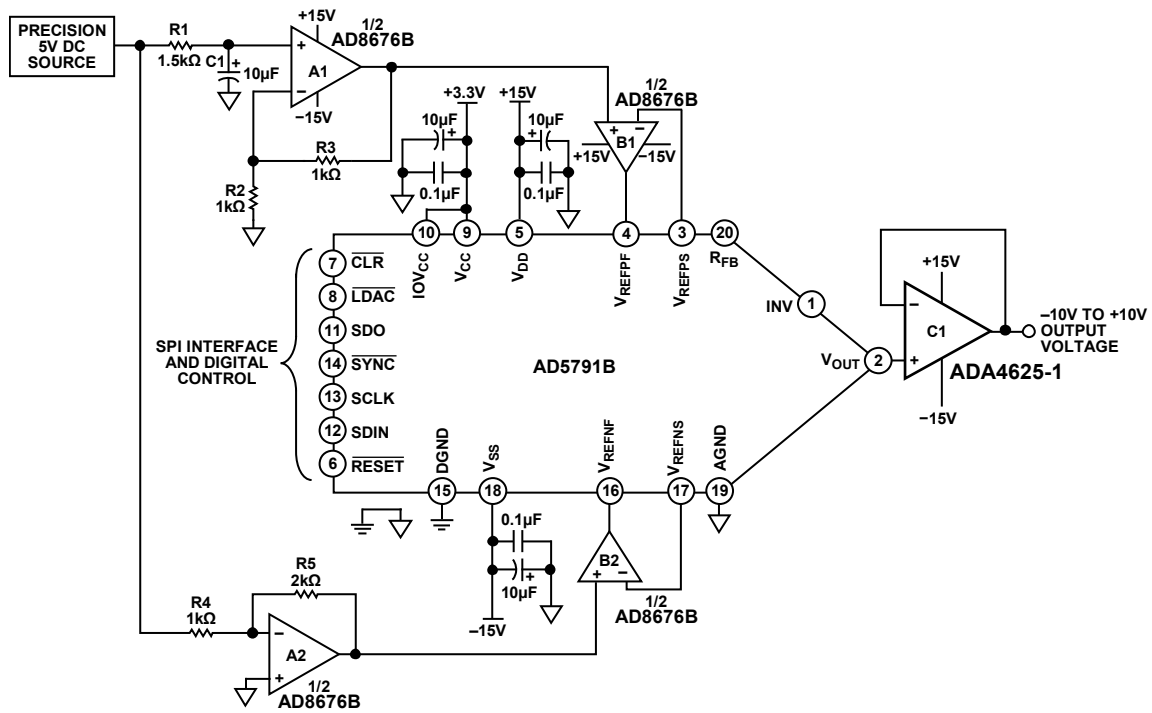


Figure 105. 20-Bit Accurate, ±10 V Voltage Source (Simplified Schematic: All Connections and Decoupling Not Shown)

ADA4625-1 can be used as an output buffer for 20-bit accurate, ±10 V voltage source with the AD5791 and the LTC6655. The low voltage noise, low drift output drive capability of the ADA4625-1, as well as dynamic parameters such as fast settling time and slew rate make the device an ideal DAC output buffer. It is recommended to provide supplies of ±15 V to obtain the full potential of the ADA4625-1 in this application due to the input V_{CM} range of the device.

Figure 106 and Figure 107 show the INL response with the EVAL-AD5791SDZ and the step response of the ADA4625-1 in comparison to the AD8675, respectively.

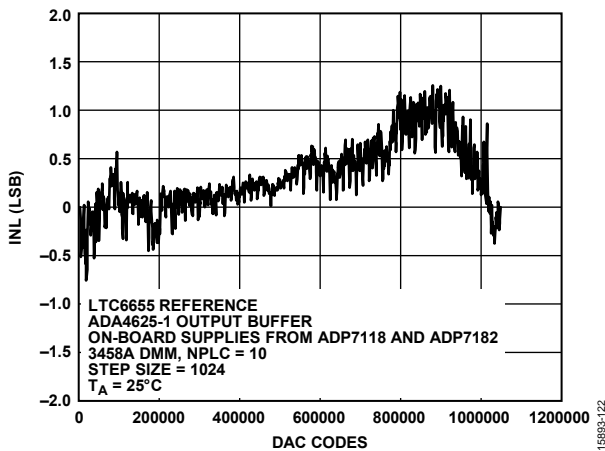


Figure 106. AD5791 with LTC6655 and ADA4625-1 as Output Buffer INL Performance

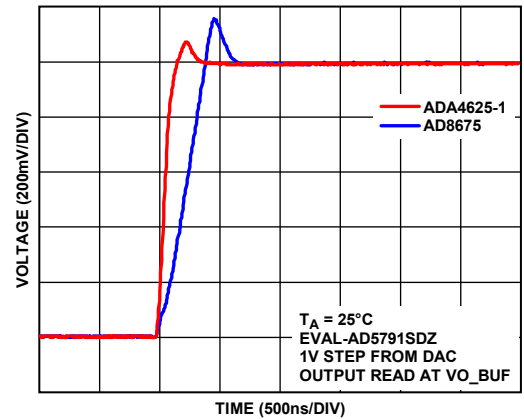


Figure 107. Step Response with ADA4625-1 and AD8675 Output Buffers

RECOMMENDED POWER SOLUTION

Analog Devices has a wide range of power management products to meet the requirements of most high performance signal chains.

For a dual-supply application, the ADA4625-1 typically needs a ±15 V supply. Low dropout (LDO) linear regulators such as the ADP7118 or the ADP7142 for the positive supply and the ADP7182 for the negative supply help improve the PSRR at high frequency and generate a low noise power rail. In addition, if a negative supply is not available, the ADP5070 can generate the negative supply from a positive supply. Figure 108 shows an example of this power solution configuration for the ADA4625-1.

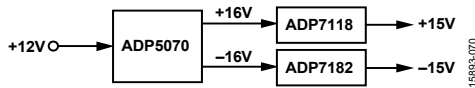


Figure 108. Power Solution Configuration for the ADA4625-1

Table 9. Recommended Power Management Devices

Product	Description
ADP5070	DC-to-dc switching regulator with independent positive and negative outputs
ADP7118	20 V, 200 mA, low noise, CMOS LDO linear regulator
ADP7142	40 V, 200 mA, low noise, CMOS LDO linear regulator
ADP7182	-28 V, -200 mA, low noise, linear regulator

It is recommended to use a low ESR, 0.1 μF bypass capacitor close to each power supply pins of the ADA4625-1 and ground to reduce errors coupling in from the power supplies. For noisy power supplies, place an additional 10 μF capacitor in parallel with the 0.1 μF for better performance.

INPUT OVERVOLTAGE PROTECTION

The ADA4625-1 has internal protective circuitry that allows voltages as high as 0.2 V beyond the supplies to be applied at the input of either terminal without causing damage. For higher input voltages, a series resistor is necessary to limit the input current. Determine the resistor value by

$$(V_{IN} - V_s)/R_s \leq 20 \text{ mA}$$

where:

V_{IN} is the input voltage.

V_s is the voltage of either V_+ or V_- .

R_s is the series resistor.

With a very low bias current of <5.5 nA up to 125°C, higher resistor values can be used in series with the inputs. A 500 Ω resistor protects the inputs from voltages as high as 10 V beyond the supplies and adds less than 2.75 μV to the offset. However, note that the added series resistor (R_s) may increase the overall noise and lower the bandwidth due to the addition of a pole introduced by R_s and the input capacitor of the amplifier.

DRIVING CAPACITIVE LOADS

The inherent output resistance of the op amp combined with a capacitive load forms an additional pole in the transfer function of the amplifier. Adding capacitance to the output of any op amp

results in additional phase lag. This lag reduces stability and leads to overshoot or oscillation, which is a common situation when an amplifier is used to drive the input of switched capacitor analog-to-digital converters (ADCs).

The ADA4625-1 has a high phase margin and low output impedance and is capable of directly driving a capacitive load up to 1 nF with no external compensation at unity-gain without oscillation.

For other considerations and various circuit solutions, see the *Ask the Applications Engineer-25, Op Amps Driving Capacitive Loads* Analog Dialogue article.

THERMAL MANAGEMENT

The ADA4625-1 can operate with up to a 36 V supply voltage with a typical 4 mA quiescent current. Heavy loads increase power dissipation and raise the chip junction temperature.

The maximum safe power dissipation for the ADA4625-1 is limited by the associated rise in junction temperature (T_J) on the die. Two conditions affect T_J : power dissipation (P_D) of the device and ambient temperature (T_A) surrounding the package. This relationship is shown in Equation 11.

$$T_J = P_D \times \theta_{JA} + T_A \tag{11}$$

where θ_{JA} is the thermal resistance between the die and the ambient environment. The total power dissipation in the amplifier is the sum of the power dissipated in the output stage plus the quiescent power. Power dissipation for the sourcing current is shown in Equation 12, where V_{SY} is the total supply voltage (V_+) – (V_-).

$$P_D = V_{SY} \times I_{SY} + ((V_+) - V_{OUT})I_{OUT} \tag{12}$$

Replace $((V_+) - V_{OUT})$ in Equation 12 with $((V_-) - V_{OUT})$ when sinking current.

For symmetrical supplies with a ground referenced load, use the following equation to calculate the average power for the amplifier processing sine signal.

$$P_{AVG,SINE} = (V_{SY} \times I_{SY}) + \left(\frac{2}{\pi} \times \frac{(V_+) \times V_{PEAK}}{R_L} \right) - \left(\frac{V_{PEAK}^2}{2 \times R_L} \right) \tag{13}$$

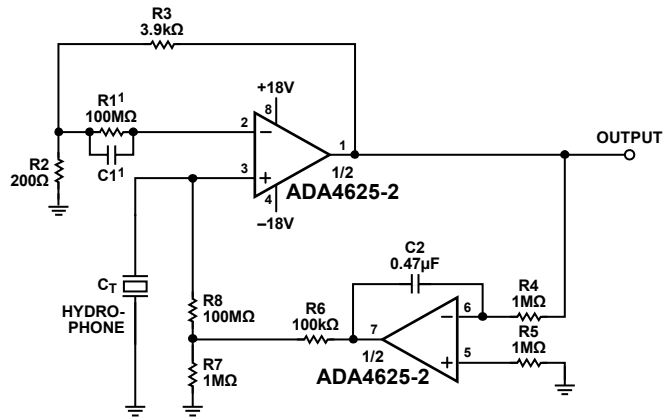
where V_{PEAK} is the peak value of a sine wave output voltage.

The specified thermal resistance θ_{JA} of the ADA4625-1/ADA4625-2 is 52.8°C/W. A good PCB layout and an external heat sink can improve thermal performance by reducing junction to ambient temperature.

The ADA4625-1/ADA4625-2 features an exposed pad that floats internally to provide the maximum flexibility and ease of use. Solder the exposed pad to the PCB board GND, or the V_+ or V_- plane for best thermal transfer. Where thermal heating is not an issue, the exposed pad can be left floating.

Incorporate the use of thermal vias or heat pipes into the design of the mounting pad for the exposed pad to lower the overall θ_{JA} .

TYPICAL APPLICATIONS

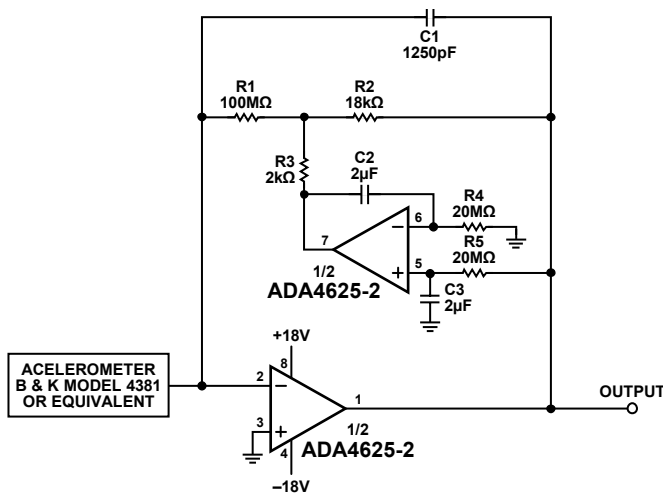


¹OPTIONAL

DC OUTPUT $\leq 750\mu\text{V}$ FOR $T_A < 125^\circ\text{C}$.
 OUTPUT VOLTAGE NOISE $\approx 128\text{nV}/\sqrt{\text{Hz}}$ AT 1kHz (GAIN = 20).
 $C1 \approx C_T \approx 100\text{pF}$ TO 5000pF ; $R4 \times C2 > R8 \times C_T$.

15893-124

Figure 109. Low Noise Hydrophone Amplifier with DC Servo



$R4 \times C2 = R5 \times C3 > R1 (1 + R2/R3) C1$.
 OUTPUT = $0.8\text{mV}/\text{pC} = 80\text{mV}/g$.
 DC OUTPUT $\leq 1\text{mV}$ FOR $T_A < 25^\circ\text{C}$.
 OUTPUT NOISE = $6.6\text{nV}/\sqrt{\text{Hz}}$ AT 1kHz.

15893-125

Figure 110. Accelerometer Amplifier with DC Servo

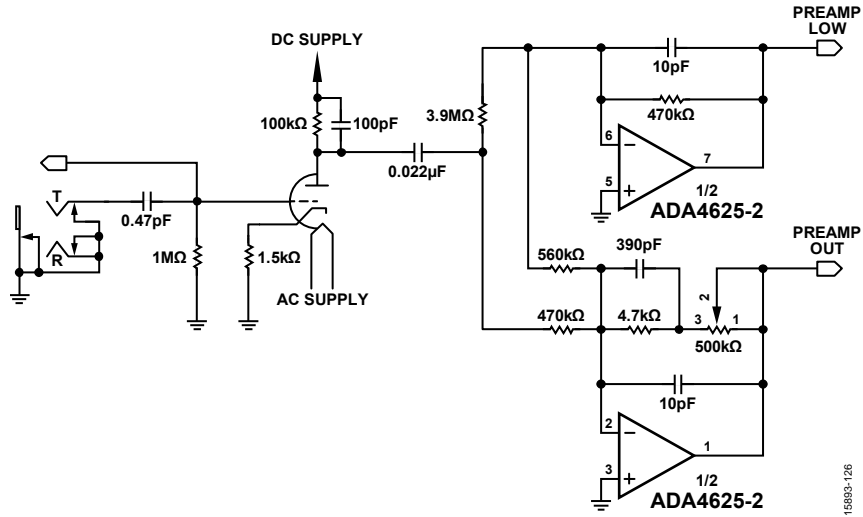
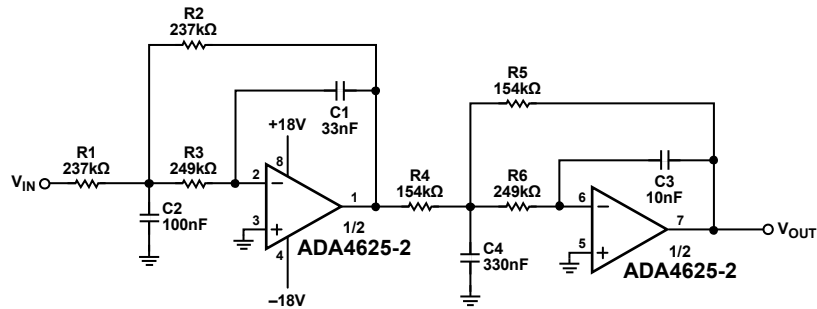


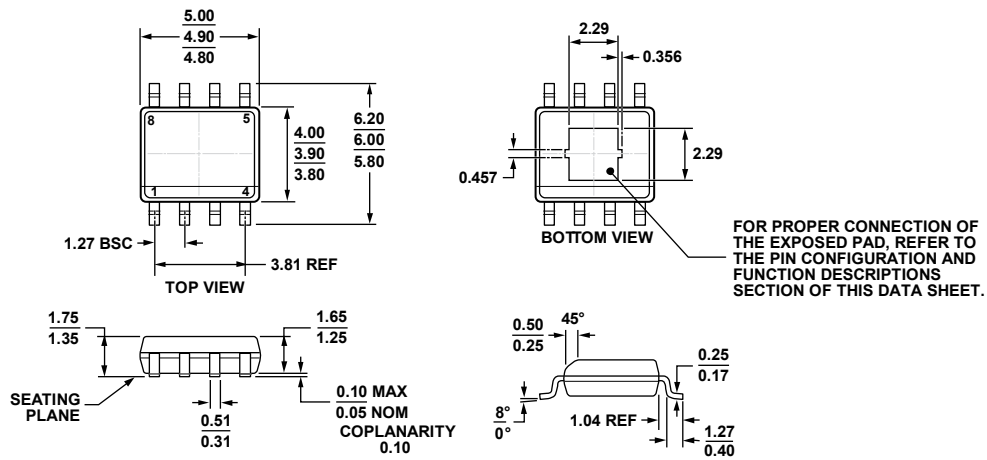
Figure 111. Guitar Preamplifier



TYPICAL OFFSET $\approx 30\mu\text{V}$.
 1% TOLERANCES
 $V_{IN} = 10\text{V p-p}$, $V_{OUT} = -110\text{dB AT } f > 300\text{Hz}$
 $V_{OUT} = -6\text{dB AT } f = 16\text{Hz}$
 THE LOW INPUT BIAS CURRENTS ALLOW THE USE OF HIGH RESISTOR VALUES.

Figure 112. 10 Hz Fourth-Order Chebyshev Low-Pass Filter (0.01 dB Ripple)

OUTLINE DIMENSIONS



COMPLIANT TO JEDEC STANDARDS MS-012-AA

Figure 113. 8-Lead Standard Small Outline Package with Exposed Pad [SOIC_N_EP]
Narrow Body
(RD-8-1)
Dimensions shown in millimeters

06-02-2011-B

ORDERING GUIDE

Model ¹	Temperature Range	Package Description	Package Option
ADA4625-1ARDZ	-40°C to +125°C	8-Lead Standard Small Outline Package with Exposed Pad [SOIC_N_EP]	RD-8-1
ADA4625-1ARDZ-R7	-40°C to +125°C	8-Lead Standard Small Outline Package with Exposed Pad [SOIC_N_EP]	RD-8-1
ADA4625-1ARDZ-RL	-40°C to +125°C	8-Lead Standard Small Outline Package with Exposed Pad [SOIC_N_EP]	RD-8-1
ADA4625-2ARDZ	-40°C to +125°C	8-Lead Standard Small Outline Package with Exposed Pad [SOIC_N_EP]	RD-8-1
ADA4625-2ARDZ-R7	-40°C to +125°C	8-Lead Standard Small Outline Package with Exposed Pad [SOIC_N_EP]	RD-8-1
ADA4625-2ARDZ-RL	-40°C to +125°C	8-Lead Standard Small Outline Package with Exposed Pad [SOIC_N_EP]	RD-8-1
EVAL-ADA4625-1ARDZ		Evaluation Board	
EVAL-ADA4625-2ARDZ		Evaluation Board	

¹ Z = RoHS Compliant Part.